Comparative & Experimental Medicine and Public Health Research Symposium

May 19 & 20, 2014

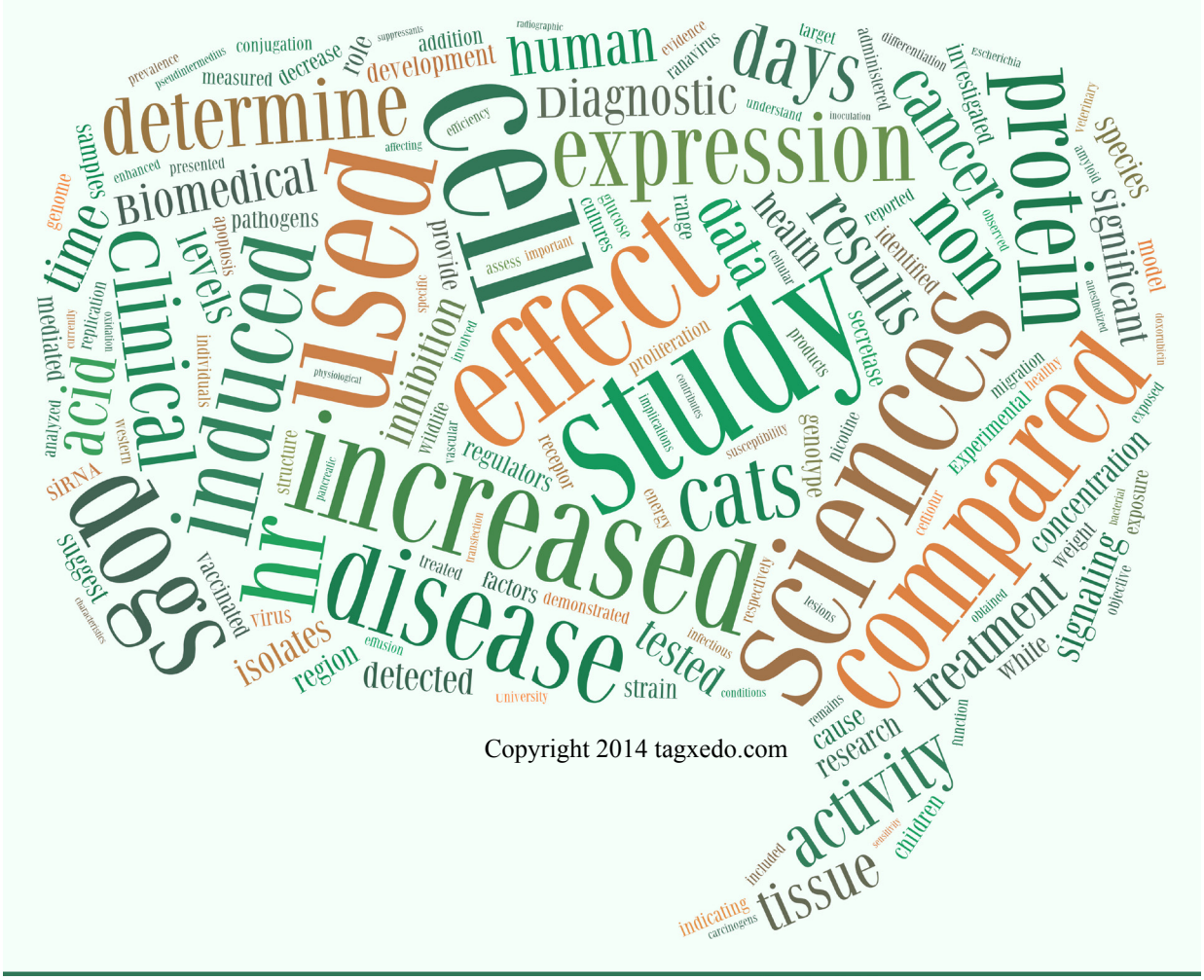

PROGRAM & SCHEDULE

Sponsored by the College of Veterinary Medicine, Department of Public Health, Tennessee AgResearch, and the UTK Office of Research

WELCOME

For the eighth consecutive year, the University of Tennessee (UT) Institute of Agriculture is hosting a symposium for UT investigators with animal and human health interests. This symposium has grown explosively and has become a calendar event for the Knoxville campuses of UT. Comparative and Experimental Medicine (CEM), an intercollegiate graduate program with shared governance by the College of Veterinary Medicine and the Graduate School of Medicine, initiated this symposium in 2007 as an event to showcase the research of CEM student investigators. In 2008, the symposium was opened to participants throughout the Knoxville campuses, and there was a four-fold increase in presentations with representation from 19 different UT departments and programs. For the sixth year, the Center for Health Policy and Services Research has teamed with CEM to produce a joint *Comparative & Experimental Medicine and Public Health Research Symposium* hosting a large group of scientists including 58 presenters representing 17 different UT departments and programs.

The *Comparative & Experimental Medicine and Public Health Research Symposium* has gained both a reputation and recognition for providing an excellent venue for students and new investigators to gain experience showcasing their work as oral presentations. In addition, the gathering of UT investigators with related and varying interests provides opportunities for the creation of new ideas, collaborations, and networking that will enhance health-related research at the UT Knoxville campuses. The joint sponsorship of the symposium by the College of Veterinary Medicine, the Department of Public Health, Tennessee AgResearch, and the UT Knoxville Office of Research signifies both a shared recognition of the need for such a symposium and a cooperative spirit in bringing this exciting event to reality.

We are happy to welcome all participants and attendees and hope the experience will be as positive as it is promising.

Larry Arrington, Chancellor
University of Tennessee
Institute of Agriculture




TABLE OF CONTENTS

We wish to acknowledge the following university programs and individuals, without whom this event would not be possible:

College of Veterinary Medicine

Department of Public Health

Tennessee AgResearch

UTK Office of Research

Misty Bailey
Kristen Bass
Michael Cunningham
Paul Campbell Erwin
Stephen Kania
Michael McEntee
Kendra L. Munsey
Kim Rutherford

We appreciate the contributions of session moderators and judges.

Thanks also to the UTCVM chapter of Phi Zeta, the UTIA chapter of Gamma Sigma Delta, the UT chapter of Sigma Theta Tau International, 2014 Center of Excellence Summer Student Research Program participants, and our sponsors and exhibitors.

Jimmy Cheek, *Chancellor*
UT Knoxville

Larry Arrington, *Chancellor*
UTIA

James Thompson, *Dean*
College of Veterinary Medicine

Taylor Eighmy, *Vice Chancellor for Research*
UT Knoxville Office of Research

William F. Brown, *Dean*
Tennessee AgResearch

Robert Rider, *Dean*
College of Education, Health & Human Sciences

Carolyn Hodges, *Dean*
UT Graduate School

SCHEDULE AT A GLANCE

Monday, May 19

	Room	Event
8:30-9:00	PBB*	Morning refreshments
9:00-10:00	156/157 PBB*	Keynote address: Jonathan Wall, PhD, "Ask Not What You Can Do with Salmon Sperm"
10:30-12:00	See session matrix (p. 6)	New investigator presentations
12:00-1:30		Break for lunch with option to purchase from UT Collegiate 4-H
1:30-2:15	Hollingsworth Auditorium	Speed networking session
2:15-4:45	See session matrix (p. 7)	New investigator presentations

Tuesday, May 20

	Room	Event
8:30-9:00	Hollingsworth Auditorium	Morning refreshments
9:00-10:00	Hollingsworth Auditorium	Plenary address: Hollie Raynor, PhD, RD, LDN "Evidence-based Practice: The Need for Efficacy and Effectiveness"
10:30-12:30	See session matrix (p. 8)	New investigator presentations
12:30-1:45		Break for lunch with option to purchase from UT Collegiate 4-H
1:45-4:15	See session matrix (p. 9)	New investigator presentations
6:00	UT Visitor's Center	Awards reception--free parking

*PBB, Plant Biotechnology Building (*see map on p. 5*)

LOCATION INFORMATION

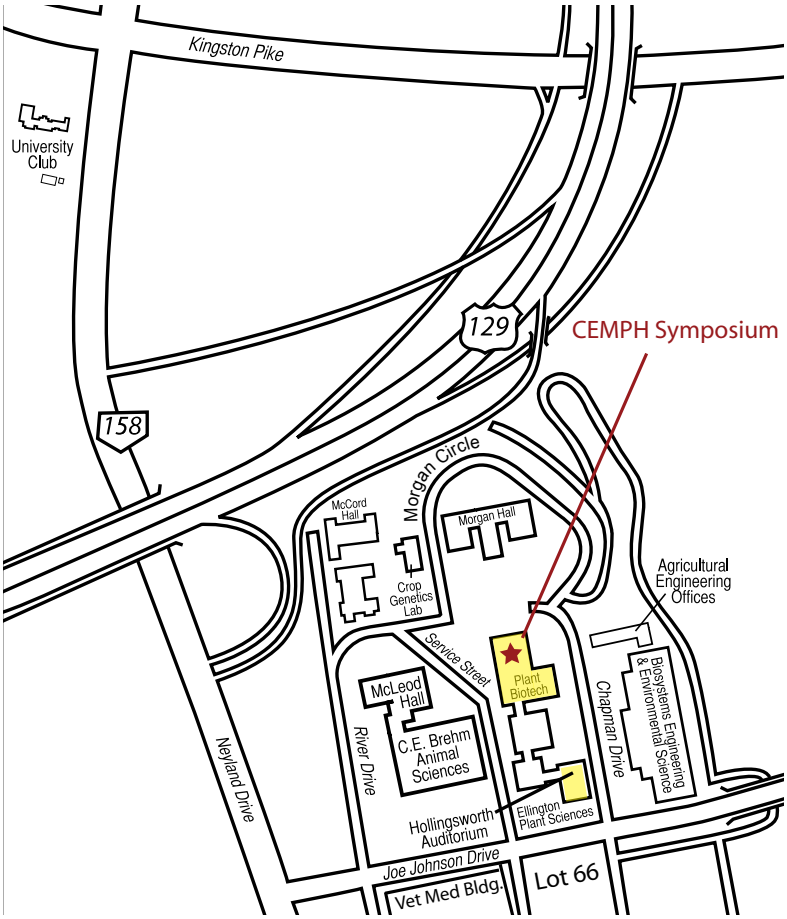

University of Tennessee Agricultural Campus

Plant Biotechnology Building

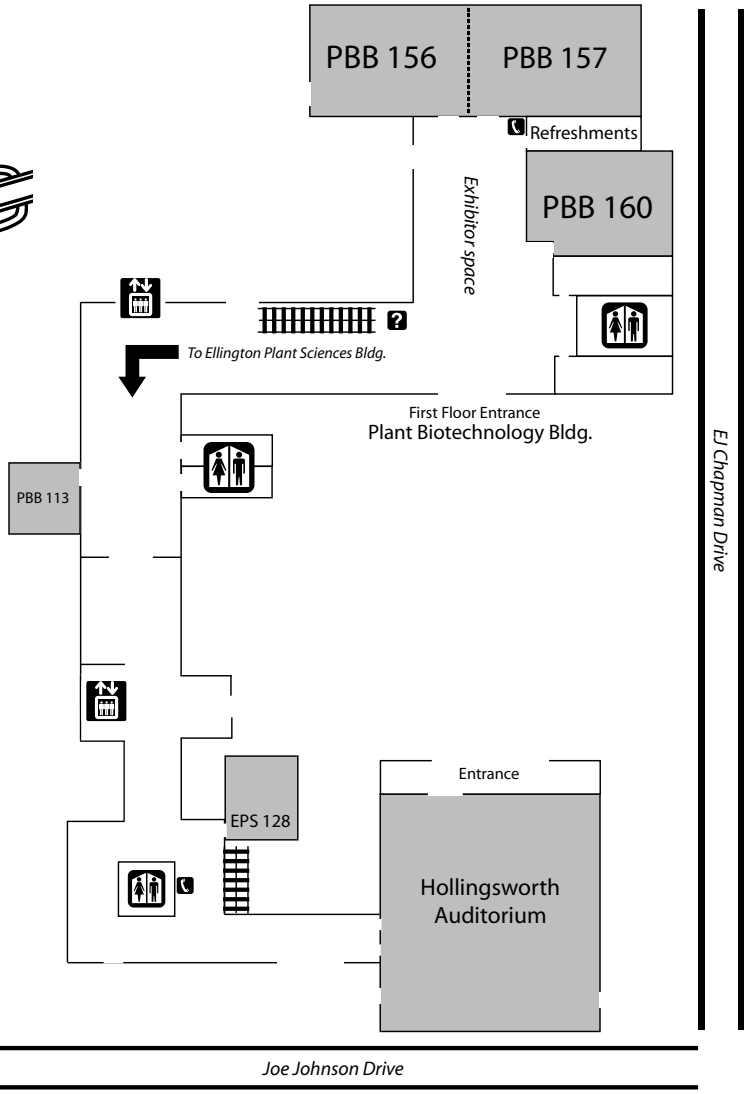

Parking

A valid student, faculty, or staff parking permit is required to park in university lots. Faculty, staff, and students with disabilities may ride a paratransit service offered by "The T" (free for all UT faculty, staff, and students) by using the Blue Phone system and requesting the Access Service. All other bus service on campus is suspended during the symposium due to no classes being in session.

__Notice__: Lot 66 may no longer be used by those without permits for that specific lot (violators may be ticketed or towed). All visitors will need a temporary parking permit.

SESSION MATRIX

Monday, May 19

(Abstracts on pp. 14-34)

9:00	**Keynote address: Jonathan Wall, PhD, "Ask Not What You Can do with Salmon Sperm" (PBB* 156/157)**	
	Clinical Sciences	**Immunology, Infectious Disease, & Molecular Biology**
	Rm. PBB* 156/157	**Rm. PBB* 160**
10:30	1. Incidence of sub-clinical middle ear effusion in dogs diagnosed during routine computed tomography **(Foster)**	19. Expression of Protein A in *Staphylococcus pseudintermedius* (**Balachandran**)
10:45	2. Evaluation of a semiquantitative SNAP test for measurement of bile acids in dogs (**Seibert**)	20. Use of siRNAs to decrease GPR54 expression in a hypothalamic neuronal cell line (**Amelse**)
11:00	3. Kinetic analysis of 2-([18F]fluoro)-2-deoxy-D-glucose uptake in brains of anesthetized healthy dogs (**Williams**)	21. Discovery and characterization of potential antifungals to treat *Candida albicans* (**Cassilly**)
11:15	4. Androgen deficiency influences matrix metalloproteinase expression and intimal hyperplasia development after vascular injury (**Freeman**)	22. Dependence of coronavirus RNA replication on an NH2-terminal partial nonstructural protein 1 in CIS (**Su** [**Brian**])
11:30	5. Use of the T2*-weighted GRE sequence for MRI examination of the canine and feline spine (**Hammond**)	23. Detection of immune modulators associated with aberrant immune response in cats infected with feline infectious peritonitis virus (FIP) (**Anis**)
11:45	6. Detection of cardiac amyloidosis by SPECT/CT imaging using both 125I-serum amyloid P-component and the novel 125I- p5R+14 peptide **(Martin)**	
12:00	**BREAK for Lunch – UT Collegiate 4-H Fund-raiser: Baked potato bar, $4**	
1:30	**Speed Networking Session (Hollingsworth Auditorium)**	

*PBB, Plant Biotechnology Building

Monday, May 19

	Clinical Sciences	Immunology, Infectious Disease, & Molecular Biology
	Rm. PBB 156/157	**Rm. PBB 160**
2:15	7. Equine mesenchymal stromal cells differentiate into cells of neural lineage: Promises for horse neuropathies (**Cruz Villagrán**)	24. *Ehrlichia* and *Rickettsia* species associations of the Gulf Coast tick (*Amblyomma maculatum*) in western Tennessee (**Mays**)
2:30	8. Comparative analysis of polymers for siRNA delivery in vascular smooth muscle cells (**Bools**)	25. Ranavirus is lethal to Boreal toad (*Bufo boreas*) tadpoles and metamorphs (**Chaney**)
2:45	11. Inotropic effect of l-lysine in healthy cats (**Johns**)	26. Flip is a novel substrate of gamma-secretase and mediates presenilin-1 induced apoptosis (**Zeng**)
3:00	**Food Safety**	27. Role of each component of gamma secretase in APP processing (**Hu**)
3:15	36. Cranberry proanthocyanidins increase reduction of a human norovirus surrogate and hepatitis A virus with increasing dose (**Sewlikar**)	28. Matricellular protein Cyr61 bridges lysophosphatidic acid and integrin pathways leading to cell migration (**Zhang**)
3:30	37. Comparison of the thermal inactivation parameters of Shiga toxin-producing *Escherichia coli* O157:H7 and non-O157 *E. coli*, in raw ground beef and turkey deli meat (**Valldares**)	**Nutrition & Metabolism**
3:45	38. Microbial control by a commercial citrus flavonoid and acid blend in liquid food models (**Techathuvanan**)	40. Impact of portion size of fruit juice on fruit juice consumption and overall energy intake during a snack in preschoolers (**Norton**)
4:00	39. *Quillaja saponaria* extract to control the spread of *Escherichia coli* O157:H7 and the emerging non-O157 Shiga toxin-producing *E. coli* (**Sewlikar**)	41. Relationship between dietary choices made during a low-calorie, low-fat diet and changes in caloric intake, caloric intake from fat, and weight loss (**Keshani**)
4:15		42. Fasting rapidly increases fatty acid oxidation in white adipose tissue (**Torchon**)

Tuesday, May 20

9:00	**Plenary address: Hollie Raynor, PhD, RD, LDN "Evidence-based Practice: The Need for Efficacy and Effectiveness" (Hollingsworth Auditorium*)**	
	Clinical Sciences	**Population Health & Epidemiology**
	Rm. PBB* 156/157	**Rm. PBB* 160**
10:30	12. A case of schistosomiasis in a young man with cyclic fevers and diarrhea (**Greer**)	43. The persistence of five *Trichomonas gallinae* isolates in simulated bird baths with and without organic material (**Purple**)
10:45	14. The interaction of magnesium sulfate and propofol on the minimum alveolar concentration preventing motor movement (MACNM) in sevoflurane-anesthetized dogs (**Johnson**)	44. Transmission of *Toxoplasma gondii* in white-tailed deer in Tennessee (**Gerhold**)
11:00	15. Role of graphene in bone tissue engineering (**Elkhenany**)	45. Wood frogs (*Lithobates sylvaticus*) may function as superspreaders of ranavirus (**P. Reilly**)
11:15	16. The effect of oral acid suppressants on intragastric pH in cats (**Parkinson**)	46. Mammary gland involution during lactation is a secondary effect of TCC-induced neonatal loss (**Kennedy**)
11:30	17. Evaluation of antibiotic concentration in a granulating wound following regional limb perfusion and systemic administration of ceftiofur (**Boswell**)	47. Prevalence of osteoarthritis in dogs undergoing routine dental prophylaxis (**Tichenor**)
11:45	18. Incidence of asymptomatic bacterial urinary tract infections in obese cats (**Mullis**)	48. Using real-time location system to investigate cattle contact structure and implications on disease transmission (**Chen**)
12:00		49. Comparing characteristics between children admitted to home health and hospice at end of life (**Lindley**)
12:15		13. Novel strain of canine distemper virus indicates possible wildlife reservoir and potential for vaccine escape (**M. Riley**)
12:30	**BREAK for Lunch – UT Collegiate 4-H Fund-raiser: Grilled cheese bar, $5**	

*Hollingsworth Auditorium, Ellington Plant Sciences Building; PBB, Plant Biotechnology Building

Tuesday, May 20

	Oncology & Cancer Cell Biology	Immunology, Infectious Disease, & Molecular Biology
	Rm. PBB 156/157	**Rm. PBB 160**
1:45	50. Chronic exposure to combined carcinogens enhances breast cell carcinogenesis with mesenchymal and stem-like cell properties (**Pluchino**)	29. Blood and milk antibody profile of dairy cows during the non-lactating and transition period (**Kerro-Dego**)
2:00	51. Piroxicam inhibits Masitinib®-induced cyclooxygenase-2 expression in oral squamous cell carcinoma cells in vitro (**Rathore**)	30. Detection and genotyping of circulating bovine viral diarrhea virus in Egyptian dairy cattle and buffalo herds (**Soltan**)
2:15	52. AD198, a derivative of doxorubicin as novel chemotherapeutic agents for treatment of transitional cell carcinoma (**Smolensky**)	31. Prevalence of *Rumenfilaria andersoni* in free-ranging moose of Minnesota (**Grunenwald**)
2:30	53. NAG-1 attenuates Smad signaling induced by TGFβ at the transcriptional level (**Min**)	32. Heat shock enhanced conjugation in *Campylobacter* (**Ardeshna**)
2:45	54. Regulation of urothelial bladder cancer by nicotine and stress neurotransmitters (**Papu John**)	33. Determining virulence factors, multi-drug resistance and typing methods of 7 *Staphylococcus pseudintermedius* clinical isolates by whole genome sequencing (**M. Riley**)
3:00	55. Nicotine-induced gemcitabine resistance is reversed by gamma-aminobutyric acid but enhanced by baclofen in pancreatic cancer xenografts and in pancreatic cancer cells in vitro (**Banerjee**)	34. The role of NLRP3 inflammasome on the pathogenesis of herpetic stromal keratitis (**Gimenez**)
3:15	**Exercise Science & Kinesiology**	35. Role of miR-155 in the pathogenesis of herpetic stromal keratitis (**Bhela**)
3:30	56. Portable indirect calorimetry systems: A review (**Wilkerson**)	
3:45	57. Financial incentives for physical activity: Effects of reinforcement schedules (**Rider**)	
4:00	58. Impact of a moderate intensity bout of walking on glucose excursions in women with gestational diabetes mellitus (**Gardner**)	
6:00	**Awards Reception (UT Visitor's Center, 2712 Neyland Drive, free parking)**	

FEATURED SPEAKERS

Jonathan Wall, PhD

Professor of Medicine
Human Immunology and Cancer Program
Director, Amyloid and Preclinical Molecular Imaging Laboratory
University of Tennessee Graduate School of Medicine

"Ask Not What You Can Do with Salmon Sperm"
Monday Keynote Address

Jonathan Wall is a tenured Professor at the University of Tennessee Graduate School of Medicine, Knoxville, TN. He graduated from the University of Essex (Colchester, UK) with a baccalaureate in biological sciences and moved to the department of Biological Chemistry and Biophysics to pursue a PhD in membrane biophysics, during which time he studied the interactions of proteins with model membrane systems under the tutelage of Prof. Paul O'Shea. After graduating, he moved to the Human Immunology & Cancer Program at the University of Tennessee Medical Center. As a post-doctoral fellow there, he worked on elucidating biochemical and biophysical aspects of immunoglobulin light chain amyloidosis. His work led to the "first-in-human" clinical trial studying the biodistribution, by using PET/CT imaging, of a novel radio-iodinated amyloid fibril-reactive monoclonal antibody in patients with light chain amyloidosis. In addition, he now leads an NIH-funded multidisciplinary team of researchers focused on developing novel therapeutic and molecular imaging agents for amyloid disease, type 2 diabetes, and cancer. In 2005, Dr. Wall was appointed Director of the Preclinical and Diagnostic Molecular Imaging Program, which specializes in using high-resolution, multi-modality micro-imaging technology for visualizing metabolic, pathologic, and anatomic features in small animal models of disease.

FEATURED SPEAKERS

Hollie Raynor, PhD, RD, LDN

Associate Professor
Department of Nutrition
Director, Public Health Nutrition
University of Tennessee

"Evidence-based Practice: The Need for Efficacy and Effectiveness"
Tuesday Plenary Address

Hollie Raynor, PhD, RD, LDN, is an Associate Professor and the Director of Public Health Nutrition in the Department of Nutrition at the University of Tennessee. She holds an MS in Public Health Nutrition and a PhD in Clinical Psychology. Dr. Raynor conducts research in lifestyle interventions for pediatric and adult weight management, has published over 80 peer-reviewed articles, and has received funding from the National Institutes of Health, American Diabetes Association, and Weight Watcher's Int., for her research. She has been selected to be a member of the National Committee for Clinical Guidelines for Obesity by the American Psychological Association. She is also a faculty member of the Academy of Nutrition and Dietetics' (AND's) Adult Weight Management certification program, serves as a member of AND's Prediabetes Evidence Analysis Library Committee, and was AND's representative to the 2014 AACE/ACE Obesity Consensus Conference.

SPEED NETWORKING

What is it?

An efficient, face-to-face professional networking model similar to "speed dating," that allows participants to make new contacts through one-on-one, focused conversations lasting 5 minutes.

Benefits of Networking

- Meeting others is a great way to find out what you might be missing.
- Making new contacts provides access to innovative, engaging colleagues who can broaden your career horizens.
- Connecting with those who have experience in fields you want to explore is an excellent way to get the inside scoop.

How it Works

- Speed networking is organized chaos--it's loud and energizing.
- Participants are split into two groups and are seated at tables in pairs facing each other. The person sitting across from you is your first partner. You spend no more than 5 minutes (2 minutes for each person and 1 minute for questions) with each partner before the signal indicates that time is up. The person on the designated side of the table is told to move one seat over to face the next person.

How to Make it a Success

- Take plenty of business cards, if you have them, and bring a pen. You may get the chance to meet more people than you expect.
- Refine your message--your 60-second story/elevator pitch (see below).
- Two minutes isn't long, so forget about listing your complete professional and personal life history. Pick a couple of key things and find an engaging way to describe them.
- Listen as well as talk.
- Remember, even if the prior or current work of the person with whom you are speaking doesn't directly relate to your interests, they might know someone who does.
- If you don't know of the other person's prior industry or organization, then ask them to clarify--otherwise, you may miss an opportunity.
- Take notes, and don't be offended if you see someone writing on the back of your business card--this practice can be very good for jogging the memory.
- Aim to network with people you haven't met before.
- If you know you want to speak with a particular person again, arrange to follow up with an e-mail/phone call to ensure they remember you.

The Elevator Pitch

A quick synopsis of your background. Your elevator speech should be brief -- no longer than 30 to 60 seconds -- the time it takes to ride an elevator, hence the name.

- Quick personal introduction
- Summarize key elements of your work and educational history and/or what you're thinking about regarding your future career path

Adapted from: https://www.gse.harvard.edu/about/administration/careers/documents/speed%20networking%20one%20page%20overview.pdf.

Abstracts

THE UNIVERSITY of TENNESSEE

Awards Descriptions

- **Graduate Student Category**: Travel awards for the top 3 presentations. 1st Place – $1,000; 2nd Place – $750; 3rd Place – $500
- **Intern/Resident Category**: Travel award for the top presentation. $1,000
- **Research Associate Category**: Travel award for the top presentation. $1,000
- **Assistant Professor Category**: Travel award for the top presentation. $1,000
- **Dr. John C. New, Jr., Award for Excellence in Public Health or Epidemiology Research:** In memory of Dr. John C. New, Jr., former professor of public health and epidemiology in the College of Veterinary Medicine. Top student presentation that demonstrates excellence in public health and/or epidemiology research. $1,000
- **Gamma Sigma Delta Award for Excellence in Agricultural & Related Sciences**: Top graduate student presentation representing Gamma Sigma Delta's high standards of scholarship in agricultural and related sciences. $250
- **Phi Zeta Award for Excellence in Animal Health Research**: Top presentation representing Phi Zeta's goal to excel in scholarship and research in matters pertaining to the welfare and diseases of animals. $250
- **Sigma Theta Tau International Award for Excellence in Human Health Research**: Top presentation that represents STTI's mission to lead using knowledge, scholarship, service, and learning to improve the health of the world's people.

1. Incidence of sub-clinical middle ear effusion in dogs diagnosed during routine computed tomography

Allison Foster, Federica Morandi, Elizabeth May
Small Animal Clinical Sciences

The objective of this study was to determine the incidence of middle ear effusion in dogs presenting for head and cervical spine imaging via computed tomography during a 2-year period. Nine dogs were referred for trauma; 102 dogs for assessment of sinonasal disease; 88 dogs for neoplastic, infectious or inflammatory disease; and 22 dogs for primary otic disease. A board-certified veterinary radiologist independently reviewed studies from 221 dogs. Radiologic evidence of middle ear effusion was identified in 22 dogs. Myringotomies were performed in seven dogs, total ear canal ablation with bulla osteotomies was performed in six dogs, and two dogs had bulla osteotomies performed. Ten of 15 cultures yielded positive growth. Negative cultures were obtained in three dogs with sterile otitis media with effusion, one dog with soft palate hypoplasia, and one dog with ceruminous gland adenocarcinoma. Fourteen of 22 dogs with middle ear effusion had chronic history of, physical examination findings consistent with, and/or radiologic evidence of otitis externa; three of 14 dogs were diagnosed with sterile otitis media with effusion via myringotomy and culture, despite having concurrent otitis externa. Of the remaining eight dogs, five had nasosinal disease, two had soft palate hypoplasia, and one had effusion associated with trauma. Statistically significant associations for middle ear effusion were present in dogs with otitis externa and soft palate hypoplasia. Neoplasia, trauma, and inflammatory/infectious disease did not significantly increase the incidence of middle ear effusion.

2. Evaluation of a semiquantitative SNAP test for measurement of bile acids in dogs

Rachel L. Seibert, Karen M. Tobias, Ann Reed, Karl R. Snyder
Small Animal Clinical Sciences

Serum bile acids (SBA) are used as a routine screening tool of liver function in dogs. Serum samples are usually shipped to a referral laboratory for quantitative analysis with an enzymatic chemistry analyzer. The canine SNAP Bile Acids Test (SNAP-BAT) provides an immediate, semi-quantitative measurement of bile acid concentrations in-house. With the SNAP-BAT, bile acids concentrations of 5 to 30 µmol/L are quantified, and results outside of that range are classified as < 5 or > 30 µmol/L. Agreement of the SNAP-BAT with the enzymatic method has not been extensively investigated. The purposes of this prospective clinical study were to assess the precision of the SNAP-BAT and determine agreement of SNAP-BAT with results from an in-house chemistry analyzer. After verifying intra-assay precision of the SNAP-BAT, a prospective analysis was performed using blood samples collected from 56 dogs suspected to have liver disease. Each sample was analyzed with an enzymatic, in-house chemistry analyzer and the SNAP-BAT. Agreement between the two methods was statistically assessed using the κ index of agreement. Intra-assay variability was minimal. The κ index for agreement between the SNAP-BAT and routine chemistry analyzer was between 0.752 – 0.819, indicating substantial to near perfect agreement. The SNAP-BAT is a highly accurate, semi-quantitative test that yields immediate results, and has very little intra-assay variability, particularly for results >30 µmol/L.

3. Kinetic analysis of 2-([18F]fluoro)-2-deoxy-D-glucose uptake in brains of anesthetized healthy dogs

Lindsay M. Williams, Federica Morandi, Dustin R. Osborne, Jill Narak, Amy K. LeBlanc
Small Animal Clinical Sciences (Williams, Morandi, LeBlanc), Department of Radiology, Graduate School of Medicine (Osborne), Department of Companion Animal Clinical Sciences, College of Veterinary Medicine, Auburn University (Narak)

Our objective was to assess kinetic 2-([18F]fluoro)-2-deoxy-D-glucose (18FDG) uptake in the brain of five anesthetized healthy adult beagle dogs by use of positron emission tomography (PET), and to determine whether 18FDG uptake differs among anatomic regions of the brain. Each isoflurane-anesthetized dog was administered 18FDG IV (dose range, 3.0 to 5.2 mCi), and PET data were acquired for 2 hr. A CT scan (without contrast agent administration) was performed to allow more precise neuroanatomic localization. Defined regions of interest within the brain were drawn on reconstructed image data. Standard uptake values (SUVs) for 18FDG were calculated to generate time-activity curves and determine time to peak uptake. Time-activity curve analysis identified four regional uptake patterns: olfactory, gray matter, white matter, and other (brainstem, cerebellum, and occipital and frontal regions). The highest maximum SUVs were identified in the olfactory bulbs and cerebral gray matter, and the lowest maximum SUV was identified in cerebral white matter. Mean time to peak uptake ranged from 37.8 min in white matter to 82.7 min in the olfactory bulbs. Kinetic analysis of 18FDG revealed differences in uptake values among anatomic areas of the brain in dogs. These data provide

a baseline for further investigation of 18FDG uptake in dogs with immune-mediated inflammatory brain disease and suggest that 18FDG-PET scanning has potential use for antemortem diagnosis without histologic analysis and monitoring response to treatment. In clinical cases, a 1-hr period of PET scanning should provide sufficient pertinent data.

4. Androgen deficiency influences matrix metalloproteinase expression and intimal hyperplasia development after vascular injury

Brian Freeman, Deidra Mountain, T. Craig Brock, Jason Chapman, Stacy Kirkpatrick, Scott Stevens, Mitchell Goldman, Frederick Klein, Michael Freeman, Oscar Grandas
Surgery, Graduate School of Medicine

Androgen deficiency (AD) is associated with increased risk of vascular disease, yet the molecular mechanisms remain unclear. Our group has previously shown testosterone regulates matrix metalloproteinases (MMP) in a dose-dependent manner in vitro. Here we investigated the role of AD & androgen replacement therapy (ART) on inflammatory cytokines & MMP-modulated intimal hyperplasia (IH) development in vivo. Aged orchiectomized (AO) rats were implanted with testosterone pellets (TST; 0.5–150 mg). ELISA & multiplex array determined serum TST & cytokine levels. Young intact (YI), aged intact (AI), & AO rats given placebo or TST supplementation underwent left common carotid balloon angioplasty following 14-day ART. Tissue samples were collected 14 days post-injury for intima:media (I:M) or MMP quantification. Therapeutic TST doses were achieved at 14 days with 0.5, 2.5, 5, and 35 mg pellets when compared to controls. Interleukin family isoforms were elevated at sub-physiological TST levels but returned to control levels with physiological TST. I:M was decreased in AI and physiological TST levels compared to YI. I:M was increased with sub- and supra-physiological TST. Injury-induced expression of MMP-2 was highest in AI and physiological TST conditions. Analysis of other MMP isoforms is ongoing. We demonstrated that low testosterone levels increase interleukin inflammatory signaling, regulate MMP expression, and increase IH development in vivo. This effect is reversed by physiologic testosterone supplementation. AD could be playing a role in vascular disease via MMP regulatory mechanisms under the control of inflammatory signaling cascades. Future studies will examine targeted inhibition of inflammatory-modulated MMP mechanisms in the prevention of dysfunctional vascular remodeling.

5. Use of the T2*-weighted GRE sequence for MRI examination of the canine and feline spine

Laura Hammond, Silke Hecht
Small Animal Clinical Sciences

T2*-weighted gradient recalled echo (GRE) is a sensitive means to detect blood degradation products and can provide additional valuable information in select cases. The goal of this study was to describe the diagnostic utility of this sequence in MRI of the small animal spine. The MRI database was searched for dogs and cats that underwent MRI studies for spinal disease in which a T2*-W GRE sequence was acquired. The scans were reviewed and the presence of susceptibility artifact recorded and characterized. The medical records were reviewed for the following: signalment, presenting symptoms, duration of clinical signs, and final diagnosis. MRI scans of 52 patients were reviewed in which susceptibility artifact was present in 39 studies on T2*-weighted images. Twenty-eight were diagnosed as intervertebral disc herniation with associated epidural hemorrhage and extruded disc material. Susceptibility artifact was also observed in cases of epidural hemorrhage associated with spinal trauma, hemophilia, and in a cystic epidural mass. The remainder of lesions displaying susceptibility artifact were intramedullary and included presumptive acute non-compressive nucleus pulposus extrusion, hematoma, hemangiosarcoma metastasis, intramedullary disc extrusion, presumptive meningomyelitis, and a mass of undetermined etiology. T2*-W GRE is a complementary sequence to standard spine MRI protocol sequences. It is useful in highlighting epidural hemorrhage associated with disc herniation and may aid in evaluation of traumatic spinal cord lesions and intramedullary lesions of uncertain origin. Inclusion of a T2*-W GRE sequence should be considered in spinal MRI when standard sequences are ambiguous or intramedullary lesions are observed.

6. Detection of cardiac amyloidosis by SPECT/CT imaging using both 125I-serum amyloid P-component and the novel 125I- p5R+14 peptide

Emily B. Martin, Tina Richey, Alan Stuckey, Craig Wooliver, Sallie Macy, Dustin Osborne, Stephen J. Kennel, Jonathan S. Wall
Comparative and Experimental Medicine (Martin), Medicine (Martin, Richey, Wooliver, Macy, Kennel, Wall), Radiology (Stuckey, Osborne, Kennel, Wall), Graduate School of Medicine

Amyloid is a pathology composed of fibrils and heparan sulfate proteoglycans that deposits in visceral organs,

leading to dysfunction and ultimately death. Amyloidosis is associated with numerous diseases. In animals, familial Shar pei fever causes renal insufficiency due to amyloidosis, and in humans, Alzheimer's disease, light chain (AL), and transthyretin (ATTR) amyloidosis are the major forms of amyloid-related disorders. Cardiac deposition of amyloid, associated with AL or ATTR, is a particularly ominous manifestation with a poor prognosis; therefore, it is critical to detect and monitor these deposits as early as possible. The amyloid imaging agent serum amyloid P component, which is used extensively in Europe, does not detect cardiac amyloid in humans and is not available for clinical use in the United States. Therefore, we have developed and validated a novel peptide that is optimized for the detection of cardiac amyloidosis in a transgenic, murine model of the disease. The peptide, designated p5R+14, is a synthetic, α-helical, 45-amino acid, heparin-binding reagent. Mice that received ~ 150 µCi of 125I-labeled p5R+14 were imaged 4 hr thereafter. A second group, injected with 125I-SAP, was imaged 24 hr post injection due to the longer serum half-life of SAP. Using both reagents, we were able to view cardiac amyloidosis in our mice. Evaluation of microautoradiography and Congo red stained-tissues confirmed that both agents localized specifically to the cardiac amyloid. Therefore, we believe that peptide p5R+14, or a similar variant, may provide a rapid, non-invasive, cost effective method for detecting cardiac amyloidosis by using PET or SPECT/CT imaging.

7. Equine mesenchymal stromal cells differentiate into cells of neural lineage: Promises for horse neuropathies

Claudia Cruz Villagrán, Lisa Amelse, Nancy Neilsen, Madhu Dhar
Comparative and Experimental Medicine (Cruz Villagrán, Amelse), Large Animal Clinical Sciences (Dhar, Amelse), Biomedical and Diagnostic Sciences (Neilsen)

Studies have shown that mesenchymal stromal cells (MSCs) are able to differentiate into extra-mesodermal lineages, including neurons. Positive outcomes were obtained after transplantation of neurally-induced MSCS (n-MSCs) in rats, rabbits, and guinea pigs after nerve injury, but potential outcomes are unknown in horses. Our objective is to evaluate the ability of equine MSCs to differentiate into cells from neural lineage, and analyze differences between horse age and cell passage number. Bone marrow-derived MSCs from young and adult horses were differentiated in nitrogen-coated dishes. After 12 hr, cells were stained to assess integrity. Protein expression of neural progenitor markers (nestin, vimentin, GFAP, β3 tubulin) was assessed via immunofluorescence and Western blot. All the cells acquired a neuron-like phenotype. Morphology of low passage cells was similar in young and adult horses; this was different with high passage cells. Nestin and vimentin were evident on undifferentiated MSCs and n-MSCs of low and high passages in both age groups; however, nestin expression in high passage n-MSCs was weaker and its location was different. Vimentin, GFAP, and β-3 tubulin on Western blot were evident on low passage extracts from young and adult horses; inconsistent results were obtained for the high passage extracts. Results reveal that equine MSCs acquire morphological and protein characteristics of neural progenitors. Ongoing studies are oriented on determining if benefits exist after transplantation of either undifferentiated MSCs or n-MSCs. The ultimate goal is to provide practical resources for treatment of neuropathies in horses.

8. Comparative analysis of polymers for siRNA delivery in vascular smooth muscle cells

Lindsay Bools, Deidra Mountain, Stacy Kirkpatrick, Josh Arnold, Scott Stevens, Mitchell Goldman, Michael Freeman, Oscar Grandas
Vascular Research Lab, Graduate School of Medicine

The use of siRNA to degrade mRNA and transiently attenuate intracellular proteins shows promise in the inhibition of vascular pathogenesis. An obstacle for application is a safe, effective delivery system due to unfavorable physiochemical properties limiting intracellular siRNA delivery. Biodegradable polymers show promise in delivering genetic material in a predictable and non-toxic way. We aim to establish polymeric transfection as a feasible non-viral, non-toxic method for gene therapy in cells of vascular origin. Human aortic smooth muscle cells were transfected in vitro with polyethylenimine and poly(B-amino ester) polymers conjugated to GAPDH or negative control (NC) siRNAs. Increasing siRNA:polymer ratios were tested for optimal efficiency. DharmaFECT2 chemical complexes were used for comparative analysis. At 24 hr post-transfection, cell toxicity was analyzed and GAPDH gene silencing was measured by qPCR normalized to 18S. Polyethylenimine-mediated transfection resulted in 81 ± 2% silencing (n = 3; $P < 0.05$ vs. NC) at 1 µg siRNA:3 µL polymer/mL. Poly(B-amino ester)-mediated transfection resulted in 90 ± 1% silencing (n = 5; $P <$ 0.05 vs. NC) at 1.35 µg siRNA:1.95 µL polymer/mL. DharmaFECT2-mediated transfection resulted in 81 ± 1% silencing (n = 4; $P < 0.05$ vs. NC) at 2.7 µg siRNA:3 µL reagent/mL. Polymeric bioconjugates transfected

HASMCs in a superior fashion to chemical complexes with comparable cell toxicity and increased silencing efficiency. Polyethylenimine bioconjugates demonstrated similar silencing efficiency to poly(B-amino ester) bioconjugates, with equivalent toxicity. Future studies will expand on polyethylenimine-mediated gene therapy for in vivo transfection in animal models of vascular disease.

11. Inotropic effect of l-lysine in healthy cats

Sara Johns, Tamberlyn Moyers, Sophy Jesty
Small Animal Clinical Sciences

The efficacy of l-lysine in controlling clinical signs of feline herpes virus is controversial, but there are no reports of side effects. A recently published study identified a positive inotropic effect of l-lysine in human, rat, and mouse myocardium in vitro. No studies have been published evaluating whether this effect is also demonstrated in vivo in these or other species. Administration of positive inotropic agents to cats with hypertrophic obstructive cardiomyopathy might worsen the hypertrophy and exacerbate the outflow obstruction, so must be undertaken with caution. We hypothesized that l-lysine would act as a positive inotrope when administered to cats at a commonly prescribed dose of 500 mg per cat twice daily. Twelve healthy adult cats were administered a commercially available l-lysine supplement at 500 mg twice daily for 90 days. Echocardiograms, blood pressures, and cardiac troponin I concentrations were evaluated before and after supplementation. No differences were detected in septal thickness ($P = 0.06$), left ventricular diastolic diameter ($P = 0.4$), left ventricular systolic diameter ($P = 0.3$), left ventricular free wall thickness ($P = 0.8$), fractional shortening ($P = 0.07$), NT-proBNP level ($P = 0.69$), or cTnI concentration ($P = 0.6$) after supplementation with l-lysine. We found no evidence that l-lysine functions as a positive inotrope in healthy cats at a dose of 500 mg twice daily. This adds to the evidence that l-lysine is safe for use in cats.

12. A case of schistosomiasis in a young man with cyclic fevers and diarrhea

Emily Greer, David Stockton, Gregory Blake, Kabir Harricharan Singh
Family Medicine, Graduate School of Medicine

A 26-year-old white male with no significant past medical history presented to the Family Medicine Clinic after developing acute, non-bloody diarrhea, cyclic fevers, and night sweats following a trip to Central Africa. Initial outpatient workup included stool studies, complete blood count, complete metabolic panel, C-reactive protein, and malaria smear, which were unremarkable aside from hemoccult-positive stool and slightly elevated CRP at 5.6. He was treated with ciprofloxacin with temporary resolution of illness. Fevers and diarrhea recurred several times, and his ciprofloxacin was increased in dosage and duration. He was then switched to amoxicillin for possible resistant strains of infectious bacteria. He was eventually admitted secondary to acute dehydration, presyncope, and persistent diarrhea. At this time his lab work was unremarkable except for an eosinophilic percentage of 45%; it would later peak at 62.4%. Aggressive intravenous fluid hydration was initiated and consults were made to infectious disease and gastroenterology. He underwent flexible sigmoidoscopy with biopsy, which was positive for *Schistosomiasis mansoni*. He received a dose of Praziquantel 3 g orally once with improvement in fevers. During his hospitalization he developed a cough; chest radiograph revealed a Löffler's pneumonia, and he was started on Levafloxacin 750 mg daily for 7 days. His discharge diagnoses included Schistosomiasis, Löffler's pneumonia, eosinophilia, thrombocytopenia, hepatosplenomegaly, and fever. He was monitored in the outpatient setting with liver function tests, stool ova and parasite, and follow-up chest radiograph. All symptoms have resolved, studies have been negative, and his eosinophilia is resolving following treatment with the Praziquantel.

13. Novel strain of canine distemper virus indicates possible wildlife reservoir and potential for vaccine escape

Matthew C. Riley, Elena Sanchez, Rebecca P. Wilkes
Comparative and Experimental Medicine (Riley), Biomedical and Diagnostic Sciences (Sanchez, Wilkes)

Canine distemper virus (CDV) is an RNA Morbillivirus capable of producing severe disease in dogs and several wildlife species. Successful vaccines have existed since the 1950s, yet clinical disease in vaccinated animals has been reported from genetically divergent strains. Recently, there has been an increase in positive samples submitted to the University of Tennessee College of Veterinary Medicine (UTCVM) Clinical Virology Lab from 5% in 2010 to 27% in 2013. Genotyping of positive CDV samples revealed a unique strain not represented before that was detected in 35/39 samples typed from Tennessee from 2011–2013, yet not detected in samples collected in 2010 (0/5). As this divergent strain was detected in both wildlife as well as three properly vaccinated dogs, we hypothesized that it could come from a wildlife reservoir and potentially be able to evade

vaccination. Genome analysis of two unrelated isolates of the new strain supported a divergent genotype while maintaining extremely low heterogeneity. In addition, preliminary serology results indicate a variable immune response between the new strain and an America-1vaccine strain. We therefore conclude that this new strain could represent a stable wildlife reservoir capable of vaccine escape.

14. The interaction of magnesium sulfate and propofol on the minimum alveolar concentration preventing motor movement (MACNM) in sevoflurane-anesthetized dogs

Alanna Johnson, Reza Seddighi, Barton Rohrbach, Sherry Cox, Christine Egger, Tom Doherty
Small Animal Clinical Sciences (Johnson, Egger), Large Animal Clinical Sciences (Seddighi, Doherty), Biomedical and Diagnostic Sciences (Rohrbach, Cox)

This study evaluated the effects of magnesium sulfate (MgSO4), alone and in combination with propofol, on the minimum alveolar concentration of sevoflurane preventing motor movement (MACNM) in dogs. Six adult male beagles (11.97 ± 1.09 kg) were anesthetized with sevoflurane on three occasions at weekly intervals using a crossover design. MACNM was defined as the minimum alveolar sevoflurane concentration preventing motor movement in response to a subcutaneous noxious stimulation (50 V, 50 Hz for 10 msec) applied to the mid-antebrachium. Baseline MACNM (MACNM-B) was determined for each anesthetic event. Treatments were administered as a loading dose (LD) and CRI as follows: T1- MgSO4 LD of 45 mg kg-1 and CRI of 15 mg kg-1 hr-1; T2- propofol LD of 4 mg kg-1 and CRI of 9 mg kg-1 hr-1; T3- MgSO4 LD of 45 mg kg-1 and CRI of 15 mg kg-1 hr-1 and propofol LD of 4 mg kg-1 and CRI of 9 mg kg-1 hr-1. Treatment MACNM determination started 60 min after initiation of the infusion. A mixed-model ANOVA was used to determine the effect of each treatment on percent decrease in MACNM-B. Data are reported as LSM ± SEM. Decrease in MACNM-B was 3.0 ± 3.1%, 48.7 ± 3.1%, and 50.3 ± 2.9%, for T1, T2, and T3, respectively. No significant difference ($P > 0.05$) existed between groups T2 and T3. Magnesium sulfate alone did not affect MACNM, nor did it potentiate the effects of propofol on MACNM.

15. Role of graphene in bone tissue engineering

Hoda Elkhenany, Lisa Amelse, Alexandru Biris, David Anderson, Madhu Dhar
Department of Surgery, Faculty of Veterinary Medicine, Alexandria University, Egypt (Elkhenany), Large Animal Clinical Sciences (Elkhenany, Amelse, Anderson, Dhar) The Center for Integrative Nanotechnology Sciences, University of Arkansas, Little Rock, Arkansas (Biris)

Engineered bone tissue has been viewed as a potential alternative to the conventional use of bone grafts, due to their limitless supply and no disease transmission. Bone tissue engineering aims to induce new functional bone regeneration via the synergistic combination of biomaterials, cells, and factor therapy. In this study, we hypothesize that graphene is a useful nanoscaffold which will promote proliferation and osteogenic differentiation of adult mesenchymal stem cells. To prove our hypothesis, we evaluated the effect of graphene, a biocompatible inert nanomaterial, on in vitro growth and osteogenic differentiation of goat adult mesenchymal stem cells. Cell proliferation and differentiation is compared between regular, polystyrene-coated tissue culture plates and graphene-coated plates. Graphitic materials are cytocompatible and support cell adhesion and proliferation. Importantly, cells seeded on oxidized graphene films undergo osteogenic differentiation in fetal bovine serum-containing medium without the addition of any specific growth factors. These findings support graphene's potential to act as an osteoinducer and a vehicle to deliver mesenchymal stem cells, and suggest that the combination of graphene and goat mesenchymal stem cells provides a promising construct for bone tissue engineering.

16. The effect of oral acid suppressants on intragastric pH in cats

Samantha Parkinson, Katherine Tolbert, Kristen Messenger, Adesola Odunayo, Mabre Brand, Ann Reed, Erin Peters, Gigi Davidson, Mark Papich
Small Animal Clinical Sciences (Parkinson, Tolbert, Odunayo, Brand, Reed), Molecular Biomedical Sciences, North Carolina State University (Messenger, Davidson, Papich), GlaxoSmithKline, Research Triangle Park, NC (Peters)

A strong correlation exists between intragastric pH and healing of gastroduodenal ulcerations in humans. Fractionated enteric-coated omeprazole and famotidine are widely prescribed acid suppressants in cats. However, once broken, the effect of enteric-coated omeprazole tablet in raising intragastric pH may be significantly

compromised. Moreover, studies have not been undertaken in cats to determine the efficacy of these different acid suppressants. The study objective was to compare the effect of acid suppressants on feline intragastric pH. Using a randomized, four-way crossover design, six healthy cats were administered famotidine, fractionated omeprazole tablet (fOT), omeprazole paste (OP) (0.88–1.26 mg/kg q12h) and placebo (lactose tablet q12h) orally for 7 days followed by a 10-day washout period. On treatment day 4, a Bravo pH capsule was placed in the stomach endoscopically and intragastric pH monitored continuously for 4 days. The mean percentage of time (MPT) that intragastric pH was ≥ 3 and 4 was compared among treatment groups using ANOVA with a post-hoc Tukey-Kramer test ($\alpha = 0.05$). The MPT ± SD the intragastric pH was ≥ 3 and 4 was 68.4 ± 35.0% and 57.8 ± 37.1% for fOT, 73.9 ± 23.2% and 55.7 ± 25.3% for OP, 42.8 ± 18.6% and 22.4 ± 14.7% for famotidine, and 16.0 ± 14.2% and 9.6 ± 10.1% for placebo. Both omeprazole formulations significantly increased intragastric pH compared with famotidine and placebo. These results indicate omeprazole fractionated tablets and omeprazole paste increase intragastric pH more effectively than famotidine or placebo and should be considered for treatment of feline acid related disorders. Fractionated enteric-coated OT is an effective acid suppressant despite disruption of the enteric coating.

17. Evaluation of antibiotic concentration in a granulating wound following regional limb perfusion and systemic administration of ceftiofur

Stacie G. Boswell, Jim Schumacher
Large Animal Clinical Sciences

Healing of wounds on the distal aspect of the limbs of horses is inhibited by infection. We can find no reports of studies quantifying the concentration of ceftiofur in granulating wounds in horses when the drug is administered by RLP or systemically. The purpose of this study was to determine the concentration of ceftiofur in granulation tissue harvested from an experimentally created wound after administering ceftiofur by regional limb perfusion (RLP) and after administering ceftiofur systemically. We hypothesized that the concentration of ceftiofur in a granulating wound would be significantly higher after RLP than after systemic administration and would be higher than its MIC; also, the concentration of ceftiofur administered systemically would be below its MIC for common pathogens. Full-thickness cutaneous wounds were created on the distal portion of two limbs of horses. Three weeks after wound creation, 1 g ceftiofur was administered either systemically though the jugular vein or as a RLP through the cephalic vein in a randomized, cross-over design with a washout period of ≥ 7 days. The concentration of ceftiofur in biopsy specimens obtained from the granulating wound at time 0, 30 min, and 2, 6, 12, and 24 hr was quantified by high-phase liquid chromatography. The concentration of ceftiofur administered systemically peaked at 2 hr and was below its MIC for common pathogens. The concentration of ceftiofur administered by RLP peaked at 30 min and exceeded its MIC for common pathogens.

18. Incidence of asymptomatic bacterial urinary tract infections in obese cats

Rebecca A. Mullis, Angela L. Witzel, Tamberlyn D. Moyers, Claudia A. Kirk, Joseph W. Bartges
Small Animal Clinical Sciences

Obesity is a growing concern in the pet population, and many feel that the severity of obesity is also increasing. A previous study (Lusby et al.) showed that obese dogs (35–44% body fat) had a 6% (1/17) incidence of asymptomatic bacterial urinary tract infections (ABUTI) while morbidly obese dogs (≥ 45% body fat) had a 31% (8/26) incidence of ABUTI. The goal of this retrospective study was to determine if obese and morbidly obese cats also exhibited an increased rate of asymptomatic urinary tract infections when compared to lean and overweight cats. Sixty-six healthy cats with varying body condition scores and urine cultures collected via cystocentesis at the time of their dual energy x-ray absorptiometry (DEXA) scans were included in the study. The cats were divided into three categories based on their body fat percentage on a DEXA scan. These categories included normal to overweight (17–34%, n = 16), obese (35–44%, n = 14), and morbidly obese (≥ 45%, n = 36) cats. None of the cats with < 45% body fat had positive urine cultures. Only one out of 36 cats with ≥ 45% body fat had a positive urine culture. In this study, the incidence of ABUTI in morbidly obese cats was 2.8%. The significance of this finding is difficult to interpret due to the small sample size, but it does not appear that obesity is a significant risk factor for ABUTI in cats.

19. Expression of Protein A in *Staphylococcus pseudintermedius*

Manasi Balachandran, Stephen Kania, David Bemis
Comparative and Experimental Medicine (Balachandran), Biomedical and Diagnostic Sciences (Kania, Bemis)

Protein A, a cell wall-associated putative virulence factor in *Staphylococcus pseudintermedius* binds IgG via its Fc region, preventing opsonophagocytic killing and thus

evades the immune system. Protein A in *Staphylococcus aureus* is also a potent B-cell superantigen which binds to VH3 B-cell receptors inhibiting antibody production. Also, B-cells undergo induced cell death with supraclonal depletion and immune tolerance upon exposure to Protein A. We hypothesize that in addition to cell wall-associated Protein A, *S. pseudintermedius* also secretes Protein A during the exponential growth phase. To test this, we investigated the presence of Protein A in culture supernatants of *S. pseudintermedius*. We first confirmed the presence of the ptaphylococcal Protein A (spa) gene by conventional PCR and sequencing. Next, we analyzed the relative expression of spa mRNA using reverse transcriptase real-time PCR assay. To detect Protein A in the culture supernatant, we developed a sensitive capture ELISA using a mouse monoclonal antibody against Protein A. The presence of Protein A in the supernatant was confirmed by Western blot. *S. pseudintermedius* isolates representing the major clonal populations in the United States were used in this study. *S. aureus* strains Cowan I, 25923 and Wood 46 were used as controls. Our results suggest that some isolates only secrete Protein A, while others secrete as well as display the cell wall-associated form. It will be interesting to investigate if the secreted Protein A differs in amino acid composition and structure from its cell wall-associated counterpart, and study its effect on B-cells.

20. Use of siRNAs to decrease GPR54 expression in a hypothalamic neuronal cell line

Lisa L. Amelse, Brian K. Whitlock
Comparative and Experimental Medicine (Amelse), Large Animal Clinical Sciences (Amelse, Whitlock)

Kisspeptin is a protein originally discovered as a human metastasis suppressor. More recently, kisspeptin and its receptor, G protein coupled receptor 54 (GPR54,) have been found to be important in the release of gonadotropin releasing hormone (GnRH) from the hypothalamus during puberty. Humans with loss of function mutations in GPR54 develop hypogonadotropic hypogonadism (HH) and do not progress through puberty. This same phenotype is seen in mice with targeted mutations in both kisspeptin and GPR54. As a tool for elucidating the pathway necessary for kisspeptin-mediated release of GnRH from hypothalamic neurons, we attempted to reduce the expression of GPR54 using siRNAs in GT1-7 cells. GT1-7 cells are a hypothalamic neuronal cell line derived from tumors in transgenic mice carrying the SV40 T antigen. Treatment with siRNA was able to reduce only GPR54 mRNA expression by 60%. Protein levels were not changed. Further studies will be done to determine if this lack of reduction in protein expression is due to the stability of the GPR54 protein in these cells and if there is any change in response to kisspeptin stimulation in cells treated with GPR54 siRNAs.

21. Discovery and characterization of potential antifungals to treat *Candida albicans*

Chelsi Cassilly, Marcus Maddox, Abigail Tester, Shawn Campagna, Richard Lee, Todd Reynolds
Microbiology (Cassilly, Reynolds) Chemistry (Tester, Campagna) St. Jude Children's Research Hospital (Maddox, Lee)

The pathogenic fungus *Candida albicans* is the leading cause of fungal nosocomial infections in immunocompromised individuals and, when involved in blood stream infections, has around a 30% mortality rate. There are currently three antifungal classes used to treat systemic infections of *C. albicans*: azoles, echinocandins, and polyenes. Rising drug resistance, as well as the toxicity of these drugs has rendered them less effective. As a result, new drugs are needed. The fungal phosphatidylserine synthase (Cho1p) has been implicated as a fungal-specific drug target because it is: 1) required for virulence in *Candida albicans*, 2) conserved among fungi, and 3) absent within mammals. To identify potential Cho1p inhibitors, a novel screen was performed on over 5,500 compounds and yielded one reproducible hit, SB-224289. This compound was tested in an in vitro PS-synthase assay and was found not to directly inhibit Cho1p. Although the compound does not directly inhibit Cho1p, it may be metabolized into a bioactive form. Structural analog analysis has revealed the active region of this compound, and lipidomic studies are under way to determine if SB-224289-treated cells have a decrease in PS levels. Further, SB-224289 could be impacting PS trafficking. A PS-specific probe is being constructed and will be used to assess any changes in PS localization based on the treatment of cells with SB-224289. This research is the first step in identifying specific and effective next generation drugs.

22. Dependence of coronavirus RNA replication on an NH2-terminal partial nonstructural protein 1 in cis

Yu-Pin Su, Yi-Hsin Fan, David A. Brian
Biomedical and Diagnostic Sciences

Viruses with an RNA genome often use stem-loop structures in the genome as signals for replication (called cis-acting signals). When the structure is disrupted,

the virus is weakened or dead, and the signal becomes a potential target for antiviral drug design. Some viral proteins involved in genome replication will also carry a cis-acting signal, and this too becomes a potential target for drug design. Here, we examine a signal of each kind that is found within a 322-nt upstream region of a replicating 2,200 nt kilobase defective RNA (also called a minigenome) of the bovine coronavirus that is not found in the otherwise identical non-replicating subgenomic messenger RNA 7. The minigenome replicates in bovine coronavirus-infected cells which provides the trans-acting factors (the RNA polymerase) for RNA replication. (i) In the first examination, mutation analyses of a recently-discovered long-range RNA-RNA base-paired structure between the 5'-untranslated region and the partial nonstructural protein1 coding region show that it is a cis-acting replication signal in the minigenome. We postulate that the higher-order structure promotes positive-strand RNA synthesis. (ii) In the second examination, multiple frame-shift, truncation, and point mutation analyses made within the partial nonstructural protein 1 coding region showed that synthesis of a PEFP core amino acid sequence within a group A-lineage betacoronavirus-conserved NH2-proximal WAPEFPWM domain is required in cis for minigenome replication. We postulate that the nascent cis-acting protein, as part of an RNA-associated translating complex, acts to direct the DI RNA to a critical site enabling RNA replication. A model is proposed that shows how this might work.

23. Detection of immune modulators associated with aberrant immune response in cats infected with feline infectious peritonitis virus (FIP)

Eman Anis, Melissa Kennedy, Alfred Legendre, Rebecca Wilkes
Comparative and Experimental Medicine (Anis), Biomedical and Diagnostic Sciences (Kennedy, Wilkes), Small Animal Clinical Sciences (Legendre); Dept. of Virology, Faculty of Veterinary Medicine, University of Minufiya, Sadat City, Egypt (Anis)

FIP is a fatal immune-mediated disease affecting cats. The pathogenesis of FIP is complicated and involves a two-pronged attack: 1) a mutant feline coronavirus (FCoV) that has the ability to infect monocytes/macrophages and 2) lack of effective host immune response (IR), which results in efficient systemic virus proliferation and the development of immune-mediated tissue destruction. This aberrant IR seems to be the result of a shift from a T helper 1 response to a T helper 2 response. Although the decisive role played by the host IR in the development of FIP is well established, little is known about the mechanism behind this response. The goal of this study was to identify the immune regulators/signals associated with FIP development. An initial screening experiment was conducted using a commercially available microarray assay for relative quantification of 84 microRNAs in paraffin embedded tissues collected from three cats that died of FIP and two cats that died from other diseases. Relative quantification of mRNA of immune regulators (PD-1, SOCS3, microRNA203) and cytokines was performed by real-time RT-PCR using total RNA extracted from peripheral blood mononuclear cells isolated from FIP-infected cats and healthy cats. MicroRNA203 and PDL-1 expression are upregulated in FIP infected cats, compared to expression from cats that died from other diseases or from healthy cats. Initial testing of other regulators and cytokines was inconclusive. Our preliminary data shows that there are multiple immune signals that may play a combined role in the aberrant IR observed in FIP infected cats.

24. *Ehrlichia* and *Rickettsia* species associations of the Gulf Coast tick (*Amblyomma maculatum*) in western Tennessee

Sarah Mays, Allan Houston, Rebecca Trout Fryxell
Entomology and Plant Pathology (Mays, Trout Fryxell), Forestry, Wildlife, and Fisheries (Houston)

The Gulf Coast tick, *Amblyomma maculatum*, is spreading from its historical range along the Gulf Coast region northward along the Mississippi River and east of the Appalachian Mountains. This tick feeds on birds and mammals, primarily cattle, and may play a role in the transmission of diseases such as rickettsiosis (*Rickettsia parkeri*) to humans, hepatozoonosis (*Hepatozoon americanum*) to dogs, and potentially Heartwater (*Ehrlichia ruminantium*) to cattle and wildlife. Gulf Coast ticks have recently been collected in western Tennessee, an area with an increased risk for Rocky Mountain Spotted Fever (*R. rickettsii*). The objective of this project is to determine the prevalence of *Ehrlichia* and *Rickettsia* spp. bacteria within questing and host-collected (cattle, deer, small mammals, and humans) *A. maculatum* from western Tennessee in 2012–2014. This will help to develop baseline prevalence and incidence data for monitoring changing *A. maculatum* populations and pathogen prevalence, and to evaluate potential threats to human and animal health. To date, the human pathogen *R. parkeri* has been identified in 23% of the questing collections. No *Ehrlichia* species have currently been identified. The identification of *R. parkeri* in the Gulf Coast tick establishes it as a vector of human concern in western Tennessee.

25. Ranavirus is lethal to Boreal toad (*Bufo boreas*) tadpoles and metamorphs

Jordan C. Chaney, Matthew J. Gray, RD Hill, J Earl, Rebecca P. Wilkes, Debra L. Miller
Center for Wildlife Health (Chaney, Gray, Hill, Miller), Biomedical and Diagnostic Sciences (Miller, Wilkes), National Institute for Mathematical and Biological Synthesis (Earl)

Ranaviruses are known to infect and cause disease in common amphibian species such as the wood frog (*Lithobates sylvaticus*). However, there is increasing evidence that rare amphibians may also be affected negatively by this emerging pathogen. For example, Mississippi gopher frogs (*L. sevosus*) and Chinese giant salamanders (*Andrias davidianus*) are highly susceptible to ranavirus. Wild populations of the boreal toad (*Bufo boreas*) have been declining for over 20 years, and pathogens are believed to play a role. To date, no studies have been performed to explore the susceptibility of boreal toad tadpoles and metamorphs to ranavirus. Thus, we exposed boreal toad tadpoles and metamorphs to an environmentally relevant concentration (103 PFU/mL) of two Frog Virus 3 (FV3)-like isolates (n = 20 tadpoles per isolate) in water and monitored survival for 21 days. Tadpoles began dying at 5 days post-exposure, and 100% mortality and infection was documented after 8 days for both isolates. Similarly, during the metamorph stage, by day 5 post-exposure, mortality and infection was 90% and 95% for both isolates. These results indicate that multiple life stages of the boreal toad are highly susceptible to ranavirus. Additionally, population simulations of wood frogs exposed to ranavirus during the larval or metamorph stage indicated extinction can occur in as fast as 5 years, if exposed every year. Such models suggest that ranavirus infection can seriously impact the federally threatened boreal toad. Future pathogen surveillance and conservation planning should consider ranavirus as a threat to this species.

26. Flip is a novel substrate of gamma-secretase and mediates presenilin-1 induced apoptosis

Linlin Zeng, Fuqiang Zhang, Chen Hu, Ting Li, Mei-Zhen Cui, Xuemin Xu
Biomedical and Diagnostic Sciences (Zeng, Zhang, Li, Cui, Xu), Comparative and Experimental Medicine (Hu)

Mutations in the presenilin 1 (PS1) gene are responsible for the majority of familial form cases of Alzheimer's disease (AD). Studies suggest that PS1 functions as the catalytic subunit of the γ-secretase complex, which is a key enzyme involved in β-amyloid peptide (Aβ) formation, a hallmark of AD. In addition to Aβ formation, PS1 has also been implicated in apoptosis. However, the mechanism by which PS1 is involved in apoptosis remains elusive. In this study, we investigated the effect of PS1 on the turnover of cellular FLICE-inhibitory protein (c-FLIP). We found that overexpression of PS1 induced apoptosis in certain types of cells and the induction of apoptosis is associated with the cleavage of c-FLIP. Our data further demonstrated that PS1-induced cleavage of c-FLICE was inhibited by γ-secretase inhibitors, but not by caspase inhibitor, indicating that cleavage of c-FLIP is catalyzed by γ-secretase. Moreover, our data also demonstrated that addition of γ-secretase inhibitors also blocked PS1-induced apoptosis. These data suggest that PS1-induced apoptosis is partially mediated by cleavage of c-FLIP. To this end, our data revealed that knockdown of caspase-8, FADD, and bid, Bax, or overexpression of Bcl-2 strongly blocked PS1-induced apoptosis, while knockdown of Bak had no effect on PS1-induced apoptosis. Knockdown of caspase-9 and SMAC at the same time also significantly inhibited PS1-induced apoptosis. In addition, our study also revealed that c-FLIP is a novel substrate of γ-secretase. These findings provide new insight into the mechanisms by which PS1 is involved in apoptosis and tumorigenesis.

27. Role of each component of gamma secretase in APP processing

Chen Hu, Ting Li, Linlin Zeng, Mei-Zhen Cui, Xuemin Xu
Comparative and Experimental Medicine (Hu), Biomedical and Diagnostic Sciences (Li, Zeng, Cui, Xu)

Based on the amyloid cascade hypothesis, the ratio of Aβ42 verses Aβ40 plays a key role in Alzheimer's disease (AD). The ratio of Aβ is controlled by gamma secretase that cleaves APP (Aβ precursor protein) at its C terminal and releases Aβ in different lengths: Aβ38, Aβ40, Aβ42, Aβ43, Aβ46, Aβ49, and so on. Hence, dissecting the biological and biochemical nature of gamma secretase is very important for understanding the mechanism of Aβ formation. Gamma secretase is a complex composed of four components: presenilins (PS1 or PS2), nicastrin (NCT), anterior pharynx-defective 1 (Aph-1), and presenilin enhancer 2 (pen-2). The roles of these components remain unclear. It is believed that all four components are required for gamma secretase activity. To be specific, PS functions as the catalytic subunit; NCT serves as a receptor for the substrate; Aph-1 is assumed to stabilize the other three components; and pen-2 was reported to be essential for the endoproteolysis of PS. However, our recent study revealed that pen-2 is dispensable for the endoproteolysis of PS, but is

required for gamma secretase activity. And in contrast to a previous study, our data demonstrate that NCT is also required for gamma secretase activity. Meanwhile, we found that APP is processed by gamma secretase in the absence of Aph-1, indicating that Aph-1 might not be required for gamma secretase activity. Furthermore, we found that post-translational modification of PS1 has strong effect on gamma secretase activity.

28. Matricellular protein Cyr61 bridges lysophosphatidic acid and integrin pathways leading to cell migration

Fuqiang Zhang, Daniel Dongwei Wu, Feng Hao, Jerold Chun, Xuemin Xu, Mei-Zhen Cui
Biomedical and Diagnostic Sciences (Zhang, Wu, Hao, Xu, Cui), Molecular and Cellular Neuroscience Department, Dorris Neuroscience Center, The Scripps Research Institute (Chun)

Lysophosphatidic acid (LPA), a potent bioactive lipid found in atherosclerotic lesions, markedly induces smooth muscle cell (SMC) migration, which is an important process in atherogenesis. Therefore, understanding the mechanism of LPA-induced SMC migration is important. Several microarray databases suggest that the matricellular protein Cyr61 is highly induced by LPA. We hypothesized that Cyr61 mediates LPA-induced cell migration. Our data show that LPA induced temporal and spatial expression of Cyr61, which promptly accumulated in the cellular Golgi apparatus and then translocated to the extracellular matrix. Cyr61 antibody blockade and siRNA inhibition both diminished LPA-induced SMC migration, indicating a novel regulatory role of Cyr61. SMCs derived from LPA receptor 1 (LPA1) knockout mice lack the ability of Cyr61 induction and cell migration, supporting that LPA1 is required for Cyr61 expression and migration. By contrast, PPARγ was not found to be involved in LPA-mediated effects. Furthermore, focal adhesion kinase (FAK), a non-receptor tyrosine kinase important for regulating cell migration, was activated by LPA at a late time frame coinciding with Cyr61 accumulation. Interestingly, knockdown of Cyr61 blocked LPA-induced FAK activation, indicating that an LPA-Cyr61-FAK axis leads to SMC migration. Our results further demonstrate that plasma membrane integrins α6β1 and αvβ3 transduced the LPA-Cyr61 signal toward FAK activation and migration. Taken together, these data reveal that de novo Cyr61 in the extracellular matrix bridges LPA and integrin pathways, which in turn, activate FAK, leading to cell migration. The current study provides new insights into mechanisms underlying cell migration-related disorders, including atherosclerosis, restenosis, and cancers.

29. Blood and milk antibody profile of dairy cows during the non-lactating and transition period

Oudessa Kerro-Dego, Raul A. Almeida, Susan I. Headrick, Mark J. Lewis, Lydia J. Siebert, Gina M. Pighetti
Animal Science (Kerro-Dego, Almeida, Headrick, Pighetti, Siebert, Oliver), ETREC (Lewis)

Streptococcus uberis intramammary infections (IMI) are increasingly prevalent, particularly in dairy herds that have controlled contagious pathogens such as *S. agalactiae*. A classical approach to control infectious disease is the use of effective vaccines; however, with bovine mastitis, this has proven particularly challenging. A critical and practical problem is to induce protective immune responses at times when dairy cows are highly susceptible to mastitis such as during the early non-lactating and peripartum periods. We vaccinated cows with *S. uberis* adhesion molecule (SUAM) and control cows with PBS at -28, 0, and 28 days relative to dry-off. Serum samples collected before each vaccination and at parturition were analyzed for presence of specific anti-SUAM antibodies. Hyperimmune serum from SUAM-vaccinated cows were used in phagocytosis and adherence/internalization inhibition assays. Results showed a steady increase in specific antibody titers in the serum and milk of vaccinated cows, which peaked after each vaccination. Further testing determined that serum anti-SUAM antibodies exert a protective effect by reducing adherence to and internalization of *S. uberis* into bovine mammary epithelial cells and by increasing phagocytosis by bovine macrophages. Antibody isotyping data of SUAM-vaccinated cows at parturition suggested IgG1/IgG2 ratio were adequate to support macrophage phagocytosis activity and this response may confer protection against *S. uberis* IMI. However, to truly assess the protective effect of *S. uberis* vaccination around dry-off, intramammary and systemic immunological profiles should be evaluated for 30 days after parturition when associated hormonal changes exert their maximum effect on the immune status of dairy cows.

30. Detection and genotyping of circulating bovine viral diarrhea virus in Egyptian dairy cattle and buffalo herds

Mohamed Soltan, Rebecca P. Wilkes, Mohamed Nagy El-sheery, Mahmoud El-heig, Melissa Kennedy
Biomedical and Diagnostic Sciences (Kennedy, Wilkes), Infectious Disease, Suez Canal University, Egypt (Soltan, El-sheery, El-heig)

Bovine viral diarrhea virus (BVDV) is one of the most economically significant diseases in the bovine industry,

with losses due to diarrhea, decreased milk production, reproductive disorders, increased susceptibility to other diseases, and mortalities. The aim of our investigation was to optimize a one-step, real-time multiplex taqman RT-PCR for diagnosis of BVDV for detection and genotyping of circulating BVDV in Egyptian dairy herds. Assay sensitivity was determined with standard RNA produced by cloning PCR products from the NADL strain, representing BVDV genotype 1, and the 125 strain, representing BVDV genotype 2, and in vitro transcription. Our optimized assay was able to detect BVDV genotype 1 and genotype 2 with an analytical sensitivity of 55 and 20 copies, respectively. A total of 397 blood and 10 aborted fetus samples were collected from four dairy cattle farms and two buffalo farms with a history of calf mortalities and/or reproductive disorders. The real-time PCR results showed 64 positive samples for BVDV genotype 1. For further subtyping of the detected viruses, a 288 bp fragment of the 5' UTR region was amplified by RT-PCR and subsequently sequenced. Phylogenetic analysis revealed BVDV genotype 1 subtype 1b. To our knowledge, it is the first report of detection of BVDV genotype 1b in Egypt.

31. Prevalence of *Rumenfilaria andersoni* in free-ranging moose of Minnesota

Caroline Grunenwald, J. Elam, E. Butler, M. Carstensen, C. Su, Richard Gerhold
Microbiology (Grunenwald, Elam, Su), Minnesota Department of Natural Resources, Forest Lake, Minnesota 55025 (Butler, Carstensen), Biomedical and Diagnostic Sciences (Gerhold)

Moose (*Alces alces*) have long been a culturally and economically valued species in Minnesota. However, over the last 8 years, the Minnesota moose population has decreased by approximately 50%. The cause of the decline is currently unclear. *Elaeophora schneideri*, a filarial parasite, is associated with moose morbidity and mortality and although not commonly reported in Minnesota, may be contributing to the population decrease. To survey for filarial parasites, moose blood and tissue samples were collected from live-caught and deceased animals. Blood was screened microscopically for the presence of microfilariae using a modified Knott's test, and all Knott's-positive animals and a negative subset were subjected to PCR with nematode-specific primers targeting the 18S rRNA gene and the first internal transcribed spacer region (ITS-1). Microscopic analysis revealed 21% (n = 226) of Minnesota moose harbored microfilariae morphologically similar to *Rumenfilaria andersoni*, a filarid previously documented in Ontario moose and associated with a peritonitis outbreak in Finnish reindeer. Accordingly, DNA sequences obtained from moose samples most closely aligned with the 18S and ITS-1 sequences of *R. andersoni*, when compared against GenBank and sequences of other known ungulate filarids. Analysis of moose samples from additional geographic locations revealed *R. andersoni* prevalence levels ranging from 21% in Maine to 64% in Alaska. This suggests the parasite is spread throughout North American moose range. At this time much is unknown about what implications, if any, *R. andersoni* has on moose health. Future research will be required to better understand the potential health implications and eco-epidemiology of this parasite.

32. Heat shock enhanced conjugation in *Campylobacter*

Devarshi Ardeshna, Ximin Zeng, Jun Lin
Animal Science

Conjugation is one of the most important horizontal gene transfer process between phylogenetically distant species in nature. Conjugation significantly contributes to the spreading of antibiotic resistance among gastrointestinal microflora. Campylobacter, the leading bacterial cause of human enteritis in developed countries, is increasingly resistant to clinical antibiotics. And the conjugation between *Escherichia coli* and *Campylobacter* species is already established. However, the mechanism, e.g., factors affecting conjugation efficiency, is still not well studied. In this investigation, *Escherichia coli* DH5α strain containing plasmid RK212.2 and shuttle vector pRY107 was constructed and used as donor of the conjugation pair. Interestingly, high temperature treatment of *Campylobacter* recipient cells dramatically increased conjugation efficiency 10–100 fold although such treatment (50°C) decreased cell viability up to 10 fold. The filtrated supernatant (potential secreted substances) from the heat shock-treated cells could not enhance the conjugation efficiency of untreated cells. Mutation in hsdR, a critical gene in Type-I methylation-restriction system, did not affect conjugation efficiency of *C. jejuni* either. In summary, heat shock of *Campylobacter* recipient cells can boost conjugation efficiency. It will help us better if we understand the mechanism of interbacterial conjugation, a significant cause of the transfer of antibiotics-resistant traits in many bacterial pathogens.

33. Determining virulence factors, multi-drug resistance and typing methods of 7 *Staphylococcus pseudintermedius* clinical isolates by whole genome sequencing

Matthew C. Riley, Stephen Kania, David Bemis
Comparative and Experimental Medicine (Riley, Kania), Biomedical and Diagnostic Sciences (Kania, Bemis)

Staphylococcus pseudintermedius is an opportunistic bacterial pathogen commonly found in dogs but capable of causing disease in other species, including humans. The prevalence of methicillin- and multi-drug resistant isolates of *S. pseudintermedius* (MRSP) is increasing, yet little is known about the transfer of drug resistance or virulence factors amongst these bacteria. Based on the lack of correlation between genetic sequence type (ST) and drug resistance profiles of our clinical collection of MRSPs, we hypothesized that drug resistance and potentially virulence factors may horizontally transfer between isolates regardless of clonal relationship. Because direct observation of a transfer event would have been difficult, we performed whole genome sequencing on multiple MRSP genomes from both related and unrelated STs to determine if novel genetic elements are clonally conserved. We observed that pan-genome analysis upheld the genetic relationships suggested by genetic typing and the majority of genome variation was due to novel distinct regions within each MRSP isolate. Most of the differences between our MRSP genomes were pathogenicity islands, drug resistance operons, prophage insertions, and plasmids. In some cases, these elements were more related to sequences from other species, and even Genera, suggesting that mobility of these elements between organisms is not a rare occurrence.

34. The role of NLRP3 inflammasome on the pathogenesis of herpetic stromal keratitis

Fernanda Gimenez, Barry T. Rouse
Comparative and Experimental Medicine (Gimenez), Biomedical and Diagnostic Sciences (Rouse)

Unraveling the initial innate events following a virus infection relates to the design of new therapies and more effective vaccines. Herpes simplex 1 (HSV-1) infection of the eye can be a cause of blindness, with lesions largely attributable to inflammatory events that include components of both adaptive and innate immunity. Several innate immune receptors are triggered by HSV-1, but it is unclear how such innate immune responses relate to the subsequent control of the virus and the ensuing inflammatory process. The present study focuses on the role of the inflammasome NLRP3, which has received minimal investigation in viral infections but is known to influence the outcome of the inflammatory disease. Unexpectedly, comparison of ocular infection with HSV-1 in WT and NLRP3 knockout (KO) mice revealed marked changes in initial events. Of interest, mice lacking NLRP3 had significantly increased early neutrophil infiltration and proinflammatory cytokines and chemokines. NLRP3 KO animals presented increased levels of mature IL-1 β and caspase 1. To explain this, we measured other innate molecules known to form inflammasomes and sense DNA viruses. Among those, we found that the nuclear sensor IFI204 is significantly more upregulated in NLRP3 KO mice compared to WT mice after HSV-1. Then, IFI204 could compensate for the absence of NLRP3, being responsible for the maturing caspase 1, IL-1β and consequently generating more aggressive disease.

35. Role of miR-155 in the pathogenesis of herpetic stromal keratitis

Siddheshvar Bhela, Barry T. Rouse
Comparative and Experimental Medicine (Bhela), Biomedical and Diagnostic Sciences (Rouse)

MicroRNAs (miRNAs) are small RNAs that regulate various cellular processes. Ocular infection with herpes simplex virus (HSV) can result in a chronic immunoinflammatory lesion that is a significant cause of human blindness. A key to controlling stromal keratitis (SK) lesion severity is to identify cellular and molecular events responsible for tissue damage. miR-155 has been identified as a critical regulator of host inflammatory responses. However, its role in immune-inflammatory reaction to infectious agents remains unclear. In this study, we demonstrated that miR-155 expression was upregulated after ocular HSV infection. Further studies showed that this increased expression of miR-155 was mainly seen in macrophages and CD4 T cells and, to a lesser extent, in the neutrophils. In vivo silencing of miR-155 by the provision of anti miR-155 (antagomir-155) nanoparticles to HSV-infected mice led to diminished SK lesions and corneal vascularization. The reduced SK lesion severity was reflected by increased SOCS1 levels and decreased production of pro-inflammatory cytokines and chemokines. Finally, miR-155KO mice were found to be resistant to herpes stromal keratitis with profound suppression of Th1 and Th17 cell responses both in the lymphoid organs and the cornea. In conclusion, our results demonstrate that miR-155 contributes to the pathogenesis of SK and may be a promising therapeutic target.

36. Cranberry proanthocyanidins increase reduction of a human norovirus surrogate and hepatitis A virus with increasing dose

Snigdha Sewlikar, Amy B. Howell, and Doris H. D'Souza
Food Science and Technology (Sewlikar, D'Souza), Marucci Center for Blueberry & Cranberry Research at Rutgers University, Chatsworth, NJ (Howell)

Plant polyphenols are gaining popularity as natural antimicrobials. Hepatitis A virus (HAV) outbreaks that cause severe foodborne disease are on the rise in the United States. Cranberry juice (CJ) and cranberry proanthocyanidins (C-PAC) have antiviral activities against human norovirus surrogates, feline calicivirus (FCV-F9), and murine norovirus (MNV-1) over 2 hr. The effects of CJ and C-PAC effects HAV are currently unknown. The objective of this research was to determine the dose and time-dependent effects on MNV-1 and HAV reduction over 24 hr at 37°C. C-PAC at 1, 2, and 4 mg/mL, CJ (pH 3.8), malic acid (pH 3.8 as control) or PBS (pH 7.2) were individually mixed with equal volumes of HAV or MNV-1 at ~5 log PFU/mL and incubated at 37°C over 24 hr. Treatments were stopped, and recovered viral titers after triplicate treatments were evaluated in duplicate by standardized plaque assays and compared to controls; data were statistically analyzed ($P < 0.05$). Transmission electron microscopy (TEM) was used to determine structural changes. CJ reduced MNV-1 and HAV to non-detectable levels after 3 hr at 37°C, while C-PAC at 1 and 2 mg/mL caused reduction of both viruses to non-detectable levels within 1 hr and 30 min, respectively. No significant reduction of MNV-1 or HAV with ethanol or malic acid controls was obtained. TEM showed structural damage of treated viruses. Increased C-PAC levels at 2 mg/mL cause higher viral reduction within shorter times. CJ and C-PAC show promise as natural antivirals against HAV and MNV-1.

37. Comparison of the thermal inactivation parameters of Shiga toxin-producing *Escherichia coli* O157:H7 and non-O157 *E. coli*, in raw ground beef and turkey deli meat

Malcond Valldares, Emefa Monu, Doris D'Souza, P. M. Davidson
Food Science and Technology

In 2012, the USDA declared non-O157 Shiga toxin-producing *Escherichia coli* as a food adulterant and included it in USDA's zero tolerance policy. Therefore, there is a need to determine this bacterium's thermal inactivation parameters. The objective of this study was to evaluate the inactivation kinetics of non-O157 cocktails compared to O157:H7 on raw and fully-cooked meat products. Five strains of individually grown O157:H7 or non-O157 were combined into two separate cocktails containing 8 log CFU/mL. Inocula were either spread onto the surface of turkey deli-meat slices or mixed with ground beef, held for 30 min, and placed into vacuum-sealed polyethylene-nylon bags. Bags were submerged in a circulating water-bath at 56°C, 58°C, or 60°C for various times, removed, and cooled in an ice bath. Blended products were serially diluted and spread-plated on tryptic soy agar plates. Survivors from three replicate experiments were enumerated after 24 hr at 37°C. D- and z-values were calculated using linear regression. In deli meat at 56, 58 and 60°C, D-values were 15.42 ± 0.08, 5.23 ± 0.16, and 1.89 ± 0.27 min, respectively, for O157:H7, and 15.48 ± 1.0, 7.20 ± 0.56, and 2.86 ± 0.22 min for non-O157. In ground beef at 56, 58, and 60°C, D-values were 11.85 ± 0.93, 5.66 ± 0.05, and 1.55 ± 0.04 min for O157:H7, and 10.59 ± 1.59, 3.30 ± 0.25, and 1.39 ± 0.29 min for non-O157, respectively. Z-values for O157:H7 and non-O157 in deli meat were 4.39 ± 0.31 and 5.46 ± 0.14°C, respectively, and in ground beef were 4.54 ± 0.24 and 4.54 ± 0.15°C, respectively. Food composition influences the thermal inactivation parameters for O157:H7 and non-O157. These data will help in designing adequate thermal processes for pathogenic *E. coli* inactivation in meat products.

38. Microbial control by a commercial citrus flavonoid and acid blend in liquid food models

Chayapa Techathuvanan, P. Michael Davidson
Food Science and Technology

Microbial control strategies are needed in the food industry to prevent foodborne illnesses/outbreaks and prolong product shelf-life. The objective of this research was to investigate the antimicrobial efficacy of a commercial naturally-derived citrus flavonoid and organic acid blend (CFA) against the foodborne pathogenic and spoilage microorganisms, *Escherichia coli, Salmonella enterica*, and *Enterobacter* spp. The antimicrobial was added to bacterial cultures in broth at 7.8–125 ppm, and growth was monitored for 48 hr at 22°C. Apple juice and milk were used as model food systems to observe the commercial antimicrobial efficacy against tested microorganisms. At 22°C, CFA at 62.5 ppm extended the lag-phase of *E. coli* for up to 24 hr. At 125 ppm, CFA caused continuous reduction of viable *S. enterica* over 24 hr. For *E. aerogenes*, 31.25-ppm CFA resulted in 1, 2.5, and 4-log reduction after 8, 24, and 48-hr exposure, respectively. In apple juice, 120-ppm CFA reduced

viable *E. coli* and *Enterobacter* spp. by at least 2 log cfu/mL, while *S. enterica* was reduced to undetectable levels (> 4-log reduction) in the presence of 180-ppm CFA in 48 hr at 22°C. When CFA was applied to milk at 12,000–18,000 ppm, no inhibition was observed in any tested microorganisms. These findings suggest that the commercial CFA is an effective antimicrobial against the foodborne bacteria tested and has potential to enhance food safety and extend product shelf-life of high-carbohydrate, low-fat, and protein foods, such as fruit-based products.

39. *Quillaja saponaria* extract to control the spread of *Escherichia coli* O157:H7 and the emerging non-O157 shiga toxin-producing *E. coli*

Snigdha Sewlikar and Doris D'Souza
Food Science and Technology

Shiga toxin-producing *Escherichia coli* (STEC) O157:H7 and the emerging big six STECs are important food safety concerns. Aqueous *Quillaja saponaria* bark extract (QE) has U.S. Food and Drug Administration approval as a food additive. QE contains bioactive polyphenols, tannins, and saponins with antimicrobial activity. The objective of this study was to determine the effects of QE against *E. coli* O157:H7 and non-O157 STECs over 16 hr at RT and 37°C. Overnight cultures of five strains of *E. coli* O157:H7 and 6 non-O157 STECs were grown in Tryptic soy broth, washed, resuspended in phosphate-buffered saline (PBS, pH 7.2), and treated with QE, citric acid (pH 3.75), sodium benzoate (0.1% w/w), or PBS (control) for 6 or 16 hr at RT and 37°C. Treatments were serially diluted and plated on Tryptic soy agar and enumerated after 24 hr. Data from triplicate treatments were statistically analyzed (ANOVA). Scanning electron microscopy (SEM) was used to determine bacterial structural changes. Reductions ranging from 0.71 ± 0.09 to 4.0 log colony forming units (CFU) were obtained for five *E. coli* O157:H7 strains treated with QE after 6 and 16 hr at RT, with increased reductions at 37°C. For six non-O157 STECs, 0.85 ± 0.12 to 2.95 ± 0.32 log reductions were obtained after 6 and 16-hr treatment with QE at RT, respectively, and at least six log reductions at 37°C. SEM analysis showed deformation in bacterial structure. QE shows antibacterial effects for potential application in food systems. Further research involves determination of the mechanism of action and evaluation in food systems.

40. Impact of portion size of fruit juice on fruit juice consumption and overall energy intake during a snack in preschoolers

Erin M. Norton, Hollie A. Raynor
Nutrition

The relationship between 100% fruit juice intake and adiposity in children may be a consequence of lack of complete compensation to energy consumed from beverages. This study investigated the impact of beverage type and beverage size on beverage and overall intake of a snack in preschool-aged children. Using a 2x2x2 design (between-subjects factor of order and within-subjects factors of beverage type [100% fruit juice vs. water] and beverage size [6 oz. vs. 12 oz.]), 26 children (3.9 + 0.6 years of age, 50% female, 73% white, and 88.5% non-Hispanic or Latino) completed snack sessions, each consisting of 200 g of applesauce, approximately 60 g of graham crackers, and either 6 oz. or 12 oz. of 100% berry fruit juice or water. Repeated measures analyses of covariance found a significant ($P < 0.05$) effect of beverage size on grams of beverage consumed and a significant ($P < 0.05$) interaction and main effects of beverage type and beverage size for beverage calories consumed. No significant difference was observed for total snack energy intake or for the energy consumed from applesauce and graham crackers between conditions. However, total caloric intake was approximately 67% higher when juice was served with the snack. Serving children larger beverage portions can lead to increased beverage intake during snack time, and leads to increased beverage energy intake if the beverage contains calories. Overall snack energy intake is also elevated when a caloric beverage is served because children do not appear to exhibit compensation to liquid calories during a snack.

41. Relationship between dietary choices made during a low-calorie, low-fat diet and changes in caloric intake, caloric intake from fat, and weight loss

Vaishali Keshani, Hollie Raynor
Nutrition

To better understand what dietary changes are related to consumption of a low-calorie, low-fat diet and improve weight loss, this secondary data analysis examined relationships between changes in food group intake and reductions in energy and fat intake and weight during a lifestyle intervention in 162 participants. Participants were aged 52.5 ± 8.4 yr, 57.4% female, and 92.0% white, with a body mass index (BMI) of

34.9 + 4.5 kg/m^2. Anthropometric and physical activity measurements and three, 24-hour dietary recalls via telephone were collected at 0, 6, and 18 months. Hierarchical regressions examined relationships between changes in food group intake and changes in energy and percent energy from fat intake and weight from 0 to 6 months (weight loss) and 6 to 18 months (weight loss maintenance). Food group intake changes with significant positive ($P < 0.05$) associations to energy and fat intake changes from 0 to 6 months were: oils, meat, fats, and dairy. Food group intake changes with significant ($P < 0.05$) associations to weight changes from 0 to 6 months were: sugar-sweetened sweets and modified lower fat sugar-sweetened fats, oils, and sweets (positive relationship); and artificially sweetened beverages and unsweetened beverages (negative relationship). Food group intake changes with significant ($P < 0.05$) positive associations to energy and fat intake changes from 6 to 18 months were nuts, fats, and modified regular fat dairy. Future research should examine if providing goals for these food groups within the context of a low-calorie, low-fat dietary prescription enhances outcomes.

42. Fasting rapidly increases fatty acid oxidation in white adipose tissue

Emmanuelle Torchon, Matthew Hulver, Ryan McMillan, Brynn Voy
Animal Science (Torchon, Voy), Virginia Polytechnic Institute, Human Nutrition, Foods & Exercise (Hulver, McMillan)

Up-regulating the fatty acid oxidation (FAO) capacity of white adipose tissue in mice protects against diet-induced obesity and excess plasma NEFA levels; however, this capacity results from the induction of brown-like adipocytes within classical white depots. Avian genomes lack a gene for uncoupling protein 1 and are devoid of brown adipocytes, making them a useful model to study lipid metabolism in white adipocytes. The objective of this study was to determine if the effects on gene expression manifested in increased rates of fatty acid oxidation. Visceral adipose tissue was collected from 21-day-old broiler chicks that were fasted for 3.5, 5, or 7 hrs, or fed ad libitum (controls). FAO was determined by measuring and summing 14CO2 production from the oxidation of [1-14C] palmitic acid. Citrate synthase activity was measured spectrophotometrically. Fasting induced a progressive increase in complete oxidation that was significantly different from controls in the 5-hr ($P = 0.0037$) and 7-hr ($P = 0.0021$) groups (1.14, 1.2, 1.49, and 1.95 nmol/mg protein/hr; control, 3.5, 5, and 7 hr, respectively). Citrate synthase activity increased significantly after 7 hr of fasting. Q-RT-PCR peroxisome proliferator activated receptor alpha (PPARα) gene fold change following a 3.5-hr (1.55) increased but decreased after 7 hr (0.78). These results confirm that fasting rapidly increases fatty acid oxidation in white adipose tissue by upregulating the transcription of key regulatory enzymes and proteins. Identifying the underlying mechanism may provide new therapeutic targets through which to increase fatty acid oxidation in situ and protect against obesity and the detrimental effects of excess NEFA on adipocyte insulin sensitivity.

43. The persistence of five *Trichomonas gallinae* isolates in simulated bird baths with and without organic material

Kathryn E. Purple, Richard W. Gerhold
Comparative and Experimental Medicine (Purple), Biomedical and Diagnostic Sciences (Gerhold)

Trichomonas gallinae, a protozoan parasite, has been implicated in recent mortality events in passerines. However, its persistence in bird baths is unknown, and these congregation sites could serve as a nidus of disease transmission. We explored the persistence of five isolates of *T. gallinae* (Cooper's hawk, broad-winged hawk, rock pigeon, Jones-barn, and house finch) in distilled water with and without the addition of untreated or autoclaved organic material. We inoculated each container with 1 x 106 trichomonads and obtained 500 mL aliquots at various time points post inoculation. Aliquots were inoculated into Diamond's media, incubated at 37°C and examined for 5 days for live trichomonads. Persistence of the isolates ranged from 0–16 hr post inoculation. The Cooper's hawk isolate persisted up 16 hr post inoculation. Persistence increased with the presence of organic material, autoclaved or untreated. We demonstrated persistence of *T. gallinae* for extended periods in simulated bird baths suggesting that contaminated bird waterers and bird baths may contribute to transmission of *T. gallinae* during outbreaks.

44. Transmission of *Toxoplasma gondii* in white-tailed deer in Tennessee

Richard Gerhold, Lisa Muller, Chunlei Su
Biomedical and Diagnostic Sciences (Gerhold), Forestry, Wildlife and Fisheries (Muller), Microbiology (Su)

Toxoplasmosis, caused by *Toxoplasma gondii*, is one of the Centers of Disease Control and Prevention's Neglected Parasitic Infections needing further research on transmission and prevention. Genotyping has disclosed

six different groups of *T. gondii* that are associated with varying degrees of virulence with some being highly virulent. Previous studies of isolates from U.S. wildlife suggest that wild species maintain a greater diversity of *T. gondii* genotypes than is found in agricultural animals; however, *T. gondii* genotype data from these hosts are limited. To further understand the diversity of *T. gondii* in white-tailed deer (*Odocoileus virginianus*), we screened sera from hunter-killed deer from eastern, middle, and western Tennessee for *T. gondii* exposure via the modified agglutination test. Heart or tongue from select seropositive animals was digested and inoculated into mice to propagate *T. gondii* tachyzoites. Tachyzoites were genotyped by multiplex multilocus nested PCR-RFLP method employing 10 genetic markers. Of the 136 sampled deer, 52 (38.2%) were seropositive. Seropositive deer were more frequent in western Tennessee (53%, n = 35) compared to middle (14.3%, n = 2) and eastern Tennessee (26.8%, n = 15). Genotyping of four white-tailed deer-derived *T. gondii* isolates disclosed type 12I isolate commonly found in wildlife in North America. We conclude that *T. gondii* is prevalent in deer in Tennessee, and further research on diversity and transmission dynamics among wildlife with these wild/feral animal genotypes is warranted. Further GIS, age, and gender analyses are being conducted to determine what factors are associated with *T. gondii* infection.

45. Wood frogs (*Lithobates sylvaticus*) may function as superspreaders of ranavirus

Patrick N. Reilly, Jordan C. Chaney, Rachel D. Hill, Debera L. Miller, Rebecca P. Wilkes, and Matthew J. Gray
Center for Wildlife Health (Reilly, Chaney, Hill, Miller, Gray), College of Veterinary Medicine (Reilly, Miller, Wilkes)

Superspreading is deemed to occur when 20% of infected individuals are responsible for > 80% of transmission. High shedding or contact rates can contribute to superspreading. The superspreading phenomenon has been identified among viruses such as HIV and SARS. Ranavirus is an emerging infectious disease shown to cause die-offs of frogs on five continents. Ranaviruses are known to infect and cause disease in common amphibian species such as the wood frog (*Lithobates sylvaticus*) and Cope's gray tree frog (*Hyla chrysoscelis*). Unknown is if certain amphibian species act as superspreading hosts, increasing the probability of a ranavirus outbreak in an amphibian community. To test this, we individually exposed 20 wood frog tadpoles and 20 gray tree frog tadpoles to an environmentally relevant concentration (103 PFU/mL) of a FV3-like isolate in 1 L of water for 3 days. Thereafter, we introduced one exposed individual to 10 unexposed individuals in a tub with water for 6 hr (n = 20 replicate tubs per species). After 6 hr, the 20 initially exposed individuals were euthanized and tissues submitted for PCR testing. The remaining individuals were separated into individual containers with 1 L of water and survival monitored for 14 days. After 14 days, superspreading was evident in all wood frog tubs. In comparison, there was no evidence of superspreading in the Cope's gray tree frog tubs. Our results suggest ranavirus transmission differs among amphibian species. Additionally, wood frog tadpoles may amplify ranavirus in aquatic systems, and perhaps increase the likelihood of infection in other species.

46. Mammary gland involution during lactation is a secondary effect of TCC-induced neonatal loss

Rebekah C. Kennedy, Laura Healy, Fu-Min Menn, Kellie Fecteau, Ling Zhao, Jiyoung Bae, Pan Hu, Nancy A. Gee, Bill L. Lasley, Jiangang Chen
Comparative and Experimental Medicine (Kennedy), Public Health (Chen), HistoTox Labs, Inc., Boulder, CO (Healy), Joint Institute for Biological Sciences & Center for Environmental Biotechnology (Menn), Biomedical and Diagnostic Sciences (Fecteau), Nutrition (Zhao, Bae, Hu), Center for Health & the Environment, University of California, Davis, CA (Gee, Lasley)

Triclocarban (TCC), an antimicrobial compound, affects pup survival during lactation in Sprague-Dawley (SD) rats. Histopathology of mammary tissue from TCC exposed dams at complete litter death revealed mammary gland involution with increased mature fat lobule separation, thinning epithelial height, alveolar ectasia, and increased epithelial vacuolation with fat. This study explores if involution is a primary outcome of TCC exposure or secondary to its effect on suckling. Pregnant SD dams (n = 6 control dams; n = 3 0.5% w/w dams) were randomized into control or 0.5% w/w TCC-treated groups from gestational day 5 (GD5) to postnatal day 6 (PND 6). Four pup substitutions with age-matched pups born and raised by control dams, were conducted. Pups were examined daily for the size of milk bands. Dams were sacrificed on PND 14, and mammary tissue was collected for histopathology evaluation. Compared to the pups born/raised by control dams, milk band scores in pups born/raised by exposed dams were similar up to PND 3 but were significantly smaller on PND 6. Histology of mammary tissue revealed no indication of involution between control and exposed dams. Our results demonstrate that mammary involution is likely an indirect effect of TCC exposure during lactation, as

mammary tissue was not involuted in exposed dams when suckling activity was maintained by continuous addition of healthy pups. This data contributes to our expanding knowledge of the effects of TCC administration during sensitive developmental periods and provides impetus for future research on the safety of TCC exposure during lactation.

47. Prevalence of osteoarthritis in dogs undergoing routine dental prophylaxis

Michelle Tichenor, Darryl Millis, Silke Hecht, Tiffany Hunt
Small Animal Clinical Sciences

It has been stated that 20% of adult dogs have osteoarthritis (OA). However, definitive data are lacking. Our purpose was to determine the prevalence of OA in dogs presented for routine dental prophylaxis. Our hypothesis was that more than 20% adult dogs would have radiographic OA. This prospective study was of 30 dogs, 4 to 10 years of age, who were presented to the UTCVM Community Practice service for dental prophylaxis. An owner questionnaire assessing function and mobility at home, weight, physical and orthopedic examination, stance and force plate gait analysis, goniometry, and sedated radiographs were collected for each dog. Average age and weight of the dogs was 7 years and 27 kg. Eighteen of 30 dogs (60%) had one or more joints with radiographic OA, with the hips and tarsi being the most commonly affected joints. Only 27% of those with radiographic OA had associated abnormalities on physical exam, while 72% were noted to be lame on an orthopedic examination. Two dogs with forelimb OA and six with hindlimb OA had decreased peak vertical force on force plate gait analysis. Owner questionnaires indicated that 12/18 dogs with OA had no clinical signs. Osteoarthritis in adult dogs appears to be more common than previously reported. Therefore, routine screening of dogs undergoing sedation or anesthesia for routine procedures is recommended in middle-aged and older dogs to allow early identification and treatment of OA that may decrease progression and improve function in dogs.

48. Using a real-time location system to investigate cattle contact structure and implications on disease transmission

Shi Chen, Brad J. White, Michael W. Sanderson, David E. Amrine, Amiyaal Ilany, Cristina Lanzas
Biomedical and Diagnostic Sciences (Chen, Lanzas), National Institute for Mathematical and Biological Synthesis (Ilany), Kansas State University (White, Sanderson, Amrine)

Location tracking systems have been widely applied in manufacturing, logistics, and other fields. However, most current systems have relatively low spatial and temporal resolution, thus dampering their feasibility in disease transmission and health management studies, where accurate estimation of contact duration and frequency plays a key role. Dairy cattle provide an ideal system because they are confined in a pen, and their position and behavior can be tracked explicitly. The real-time location system (RTLS) that we propose to implement can collect cattle position data with high precision (up to 0.01 m) and accuracy (up to 0.1 m) at a 1-sec resolution. These originally reported location data can be further transformed to contact network data for both animal-animal contact and animal-environment contact, to assess their implications on disease transmission and herd management using a combination of computational methods and modeling techniques. From this project, we expect to get a comprehensive understanding of dairy cow contact structure and implications on health research, collaborate with researchers from various disciplines, train students and veterinarians, help farm workers and managers, and inform public health administrators.

49. Comparing characteristics between children admitted to home health and hospice at end of life

Lisa C. Lindley
Nursing

Home health care and hospice care offer terminally-ill children and their families different care models at end of life. Differences exist in the rules and regulations that govern delivery of care (e.g., intermittent short-term need vs. 6-month prognosis) and the focus of care at end of life (e.g., restorative vs. comfort). Yet, little is known about the children who are admitted to home health and hospice care. The purpose of this study was to analyze differences in the characteristics between children admitted to home health and hospice at end of life. Participants were a cohort of 370 pediatric decedents from the California Medicaid claim files, a pooled cross-sectional dataset from 2007 and 2008. Using the Andersen Model of Health Services Use as a framework, a descriptive analysis was conducted to compare predisposing, enabling, and need characteristics between children admitted to home health and hospice in the last year of life. A majority of terminally-ill children were admitted to home health (83.8%). Compared to hospice, home health children were often toddlers between the ages of 1 and 5 years (39.0%), who were

Medicaid eligible because of family income (84.8%) and frequently had serious complex chronic cardiac (45.5%) and gastrointestinal (16.1%) conditions with four or more medical comorbidities (19.7%). Understanding the unique characteristics of children admitted to home health and hospice care may be essential for advancing knowledge and compassion for children and their families at end of life.

50. Chronic exposure to combined carcinogens enhances breast cell carcinogenesis with mesenchymal and stem-like cell properties

Lenora A. Pluchino, Hwa-Chain Robert Wang
Genome Science and Technology (Pluchino), Biomedical and Diagnostic Sciences (Wang)

Most breast cancers are attributable to chronic exposure to low doses of multiple carcinogens. To understand how multiple carcinogens act together to induce breast cell carcinogenesis, we studied the activity of 4-(methylnitrosamino)-1-(3-pyridyl)-1-butanone (NNK), benzo[a]pyrene (B[a]P) and 2-amino-1-methyl-6-phenylimidazo[4,5-b]pyridine (PhIP) using our chronically induced cellular carcinogenesis model. NNK is a tobacco-specific nitrosamine ketone, and B[a]P is an environmental polycyclic aromatic hydrocarbon; both are weak mammary carcinogens in humans. PhIP is a heterocyclic amine derived from high-temperature cooked meats with known implications for human breast cancer. Given the ubiquitous nature of tobacco smoke, carbon exhaust and cooked meats in most societies, it is important to examine how relatively weak environmental breast carcinogens can augment the potential of a potent dietary breast carcinogen. Results revealed, for the first time, that combined NNK and B[a]P enhanced cellular carcinogenesis chronically induced by PhIP in both non-cancerous and cancerous breast cells. Co-exposure was more potent than sequential exposure in initiation of cellular carcinogenesis measured by transient induction of DNA damage, reactive oxygen species elevation, ERK pathway activation and increased cellular proliferation, and progression of carcinogenesis measured by acquisition of various cancer-associated properties including enrichment of stem-like cell population and activation of the epithelial-to-mesenchymal transition program. Using our model as a target, we detected that a combination of the green tea catechins ECG and EGCG, at non-cytotoxic levels, was more effective than individual agents in intervention of cellular carcinogenesis induced by combined carcinogens.

51. Piroxicam inhibits Masitinib-induced cyclooxygenase-2 expression in oral squamous cell carcinoma cells in vitro

Kusum Rathore, Mary-Mc Alexander, Maria Cekanova
Small Animal Clinical Sciences

Development and characterization of animal models for human cancers is important for the improvement of diagnosis and therapy. The oral squamous cell carcinoma (OSCC) of domestic animals resembles human OSCC in many aspects; therefore, cell lines derived from OSCC of cats and dogs are a valuable model for studying human OSCC. Here, we characterized one feline (FeOSCC-Sidney) and one canine OSCC (K9OSCC-Abby) cell line and compared their characteristics with the human OSCC cell line SCC-25. We calculated the proliferation doubling time of new OSCC cell lines and evaluated the expression profiles of cancer-related markers and cell-cycle proteins like c-kit, PDGFR, VEGFR, EGFR, COX-1, COX-2, and p27 by immunocytochemistry and Western blotting analysis. We evaluated the effects of novel receptor tyrosine kinase inhibitor (RTKI, Masitinib, AB1010) alone or in combination with a non-steroidal anti-inflammatory drug (piroxicam) on OSCC cells. Interestingly, AB1010 increased expression levels of cyclooxygenase-2 (COX-2) in all tested OSCCs. When compared to either drug alone, co-treatment of piroxicam with Masitinib significantly inhibited proliferation of tested OSCCs cells through inhibition of c-kit and AKT signaling pathways. In addition, piroxicam inhibited Masitinib-induced COX-2 expression in all tested OSCCs. Therefore, targeting COX-2 and PDGFR/c-kit signaling pathways simultaneously was more efficient for inhibition of OSCCs across these species. Although Masitinib inhibited RTKIs and OSCC cell proliferation, it stimulated the expression of COX-2. This might be one possible mechanisms of the drug-resistant effects of RTKIs. This finding demonstrates the need for careful use of RTKIs in human and veterinary cancer patients.

52. AD198, a derivative of doxorubicin as novel chemotherapeutic agents for treatment of transitional cell carcinoma

Dmitriy Smolensky, Kusum Rathore, Maria Cekanova
Graduate School of Genome Science and Technology (Smolensky), Small Animal Clinical Sciences (Rathore, Cekanova)

Transitional cell carcinoma (TCC) is a one of the most common cancers in the urinary tract system. The location of TCC can often be a limiting factor for surgery and/

or radiation. Doxorubucin has been one of the main effective chemotherapy agents used for treatment of TCC. However, some patients are not appropriate candidates to receive doxorubicin because of its cardio-toxic effects and/or the development of drug-resistance to doxorubicin. In this study, we have evaluated effects of a novel derivative of doxorubicin, AD198, in human T24, UMUC-3, and canine primary TCC cell lines. AD198 does not show cardio-toxicity as compared to parental doxorubicin in rodents. The lipophilic structure of AD198 allows it to enter the cells through cell membrane diffusion, without the use of influx transporters. Unlike doxorubicin, which has several nuclear targets, AD198 activates protein kinase C delta to induce apoptosis. In this study, we showed that AD198 more significantly inhibited cell proliferations of TCC as compared to doxorubicin in both canine and human TCC cell lines. The mechanisms of AD198 action in bladder TCC are currently under intensive investigation.

53. NAG-1 attenuates Smad signaling induced by TGFβ at the transcriptional level

Kyung-Won Min, Jason Liggett, Wells W. Wu, Rong-Fong Shen, Seung Joon Baek
Comparative and Experimental Medicine (Min), Biomedical and Diagnostic Sciences (Liggett, Baek), Facility for Biotechnology Resources, CBER, Food and Drug Administration, Bethesda, MD (Wu, Shen)

Non-steroidal anti-inflammatory drug (NSAID)-activated gene (NAG-1) is a divergent member of the transforming growth factor-beta (TGF-β) superfamily, which are key regulators of metazoan embryo development and adult tissue homeostasis. Abberant regulation of TGF-β signaling can contribute to various diseases such as cancer. Although there is sequence similarity between NAG-1 and other TGFβ superfamily members, NAG-1 does not bind to the TGFβ receptors. The biological consequence of NAG-1 remains to be elucidated. It has been known that NAG-1 is regulated via the tumor suppressor gene p53 or early growth response-1 (EGR-1), or via the PI3K/AKT/GSK-3β pathway. Unlike the transcriptional regulation of NAG-1, the principal function, receptor, and signaling pathway of NAG-1 remain uncertain, and the biological role of NAG-1 in tumorigenesis remains poorly understood and sometimes contradictory. Here, we conducted transcriptome analysis to study downstream effects and/or pathways. We employed comparative RNA-seq (next generation sequencing) profiling of the transcriptomes under two different conditions: normal U2OS and NAG-1 over-expression U2OS cells. RNA-seq results revealed 142 differentially expressed genes, 19 of which have been reported as TGF-β1 target genes, implying that NAG-1 may crosstalk with TGF-β1 signaling. NAG-1 modulates TGF-β1 signaling without affecting Smad2 phosphorylation. NAG-1 seems to interrupt the Smad complex and thus interrupts binding to the promoter region containing Smad binding elements. Overall, this study provides new evidence that NAG-1 controls transcriptional regulation in the Smad pathway.

54. Regulation of urothelial bladder cancer by nicotine and stress neurotransmitters

Arokya Mary Sashi Papu John, Jheelam Banerjee, Hildegard M. Schuller
Biomedical and Diagnostic Sciences

Urothelial bladder cancer (UBC) is the seventh most common cancer in men and the seventeenth most common cancer in women. Smoking is an established risk factor for UBC. However, the mechanisms of how smoking induces bladder cancer are poorly understood. Using two established human urothelial bladder cancer cell lines, our data show that nicotine significantly increased the proliferation of both cell lines. Both cell lines produced the stress neurotransmitters norepinephrine and epinephrine, and nicotine further enhanced this activity. The broad-spectrum beta-blocker propranolol strongly inhibited base-level and nicotine-induced proliferation in both cell lines, identifying beta-adrenergic receptors as mediators. Proliferation in response to exogenous addition of epinephrine, norepinephrine, or the selective beta-adrenergic agonist isoproterenol and complete blockage of these responses by propranolol support this interpretation. Treatment with the inhibitory neurotransmitter gamma aminobutyric acid (GABA), which inhibits beta-adrenergic receptor-mediated proliferation of other cancer types via inhibition of cAMP formation, was less effective. These findings suggest that urothelial bladder cancer cells are stimulated in their growth via beta-adrenergic receptor signaling independent of cAMP by nicotine or psychological stress. Additional investigations are underway to further dissect the signal transduction pathways involved.

55. Nicotine-induced gemcitabine resistance is reversed by gamma-aminobutyric acid but enhanced by baclofen in pancreatic cancer xenografts and pancreatic cancer cells in vitro

Jheelam Banerjee, Hussein A. N. Al-Wadei, Mohammed H. Al-Wadei, Koami Dagnon, Hildegard M. Schuller.
Biomedical and Diagnostic Sciences (Banerjee, HAN Al-Wadei, Dagnon, Schuller), Comparative and Experimental Medicine (MH Al-Wadei)

Pancreatic cancer is frequently resistant to cancer therapeutics. Smoking and alcoholism are risk factors, and pancreatic cancer patients often undergo nicotine replacement therapy (NRT) and treatment for alcohol dependence. Based on our report that low-dose nicotine within the range of NRT causes gemcitabine resistance in pancreatic cancer, our current study has tested the hypothesis that GABA or the selective GABA-B-R agonist baclofen used to treat alcohol dependence reverses nicotine-induced gemcitabine resistance in pancreatic cancer. Using pancreatic cancer cell lines BXPC-3 and PANC-1, our data show that GABA significantly reversed gemcitabine resistance induced by low-dose nicotine in xenografts, whereas baclofen did not. This effect of GABA was accompanied by decreases in cAMP, p-CREB, p-AKT, p-Src, p-ERK metalloproteinases-9 and -2, and EGR-1, and increases in cleaved caspase-3 in xenografts, whereas baclofen had opposite effects. In vitro exposure of cells to single doses or 7 days of nicotine induced protein expression of MMP-2, MMP-9, and EGR-1, and these responses were blocked by GABA. Baclofen downregulated the protein expression of GABA-B-Rs in xenograft tissues and in cells exposed to baclofen for 7 days in vitro. This response was accompanied by inversed baclofen effects from inhibition of cAMP formation after single-dose exposures to stimulation of cAMP formation in cells pretreated for 7 days. These findings suggest GABA as a promising agent to overcome nicotine-induced gemcitabine resistance in pancreatic cancer whereas treatment of alcoholism by baclofen may increase gemcitabine resistance. Supported by grants R01CA130888 and R01CA042829 with the National Cancer Institute.

56. Portable indirect calorimetry systems: A review

Brittany S. Wilkerson, David R. Bassett, Jr., Scott E. Crouter, Brian C. Rider, Brian B. Parr
Kinesiology, Recreation, and Sport Studies (Wilkerson, Bassett, Crouter, Rider), Exercise and Sports Science, University of South Carolina Aiken (Parr)

The purpose of this study was to summarize the historical development of portable indirect calorimeters, describe their principles of operation, and report on their validity and reliability. Ten devices were selected for review: the Kofranyi-Michaelis (KM), Oxylog, Aerosport TEEM 100 (TEEM), Aerosport KB1-C (KB1-C), Cosmed K2 (K2), VmaxST/Metamax3B, Medgraphics VO2000, Cosmed Fitmate (Fitmate), Cosmed K4b2 (K4b2) and the Oxycon Mobile (Oxycon). The validity of each device for measuring oxygen uptake (VO2) was compared to the gold standard Douglas bag method (DBM) at rest, moderate exercise (e.g., 150 Watts), and vigorous exercise (e.g., ≥200 W or VO2max). The mean percent errors in VO2 measurements ranged from -53% (VO200) to +82% (KB1-C) with the greatest variations observed at rest. At moderate work rates, mean percent errors ranged from -4.6% (K2) to +9% (VO2000). At high work rates or maximal exercise, mean percent errors ranged from -5.9% (KB1-C) to +11.8% (VmaxST). Over time, indirect calorimeters have become lighter, more sophisticated, and more comfortable to wear. The validity of these devices varies; however, a number of these systems provide valid estimates of VO2 (mean values within 5% of DBM) during exercise and sport activities.

57. Financial incentives for physical activity: Effects of reinforcement schedules

Brian C. Rider, David R. Bassett, Dixie L. Thompson, Eugene C. Fitzhugh, Hollie Raynor, Shannon Looney
Kinesiology, Recreation, and Sport Studies (Rider, Bassett, Thompson, and Fitzhugh), Nutrition (Raynor and Looney)

The purpose of this study was to compare the effects of two different financial incentive reinforcement schedules on daily step goal compliance, within the context of a minimal contact, lifestyle intervention. Fifty-seven adults (89% female; age 49.6 + 9.0 yr) were randomized into incentive group 1 (G1, N = 29) in which participants received $1.00 for each day they met their step goal (money paid at the end of the program) and incentive group 2 (G2, n = 28) in which participants received a fixed enrollment incentive of $70 at the beginning of the program. They were instructed to increase daily steps by 1,000; 2,000; and 3,000 steps/day over their individual baseline steps for week 1, week 2, and weeks 3–12, respectively. Intention-to-treat analysis revealed no significant difference between groups in the average daily step count ($P > 0.05$). There were no between-group differences in step goal compliance (G1 59% vs. G2 51% of meeting daily step goal, $P > 0.05$) or weight.

Steps/week increased significantly for both groups from baseline (G1 = 4549 ± 1366 to 6839 ± 2852 steps G2 = 4524 ± 1171 to 6549 ± 2463 steps, $P < 0.05$), but there was no significant difference between groups ($P > 0.05$). The present study confirms that a minimal contact lifestyle intervention was effective for increasing ambulatory PA and promoting weight loss. Both incentive reinforcement schedules were equally effective in impacting daily step compliance.

58. Impact of a moderate intensity bout of walking on glucose excursions in women with gestational diabetes mellitus

Doree Lynn Gardner, Jennifer White, Dawn P. Coe
Kinesiology, Recreation, and Sport Studies

Gestational diabetes mellitus (GDM) is a form of glucose intolerance during pregnancy. Research shows that postprandial glucose levels may have a greater impact than fasting glucose on maternal and fetal health. A postprandial glucose excursion (PPGE) is defined as the change in glucose concentration from before meal to after meal. No study has investigated the impact of physical activity on PPGEs in women with GDM. The purpose of this study was to determine the impact of a bout of moderate intensity walking on PPGEs in women with GDM. Subjects were seven women with GDM (29.2 ± 5.1 yr). Each woman wore a continuous glucose monitoring system (CGMS) for 5 days. Two randomly assigned conditions were compared: 30 min moderate intensity treadmill walking (80 m•min-1, WALK) versus 30 min sitting (CON). These assessments were completed 48 hr apart. Data extracted from the CGMS were used to determine the number of PPGEs, peak PPGE, and average glucose difference during the PPGE. Paired *t* tests were used to determine differences in these variables between the WALK and CON days. There were no significant differences for any of the variables across conditions. However, there was a trend for significance for number of PPGEs and average glucose difference during the PPGEs. There was a trend for fewer PPGEs during the walk day (1.9 ± 0.3 vs. 2.6 ± 0.3; $P = 0.09$). The average glucose difference during the PPGE was somewhat lower on WALK day (41.4 ± 6.3 mg/dL vs. 52.5 ± 5.8 mg/dL; $P = 0.07$). Moderate intensity walking may attenuate the number and intensity of PPGEs in women with GDM.

Notes:

Sponsor & Exhibitor Directory

Charles River Laboratories
Lorie Boyd
(919) 723-8356
lorie.boyd@crl.com

Fisher Scientific
Chuck Edrington
(865) 406-3371
chuck.edrington@thermofisher.com

Pendergrass Library (Agriculture & Veterinary Medicine), UT
Ann Viera
(865) 974-9015
annviera@utk.edu

Thermo Fisher
Brent Krugh
(615) 715-9835
brent.krugh@thermofisher.com

UT Federal Credit Union
Teri Branam
(865) 971-1971 (Ext. 115)
tbranam@utfcu.org

UTIA Sponsored Programs Office
Debbie Hampstead
(865) 974-7357
aggrant@utk.edu